






Astrocyte-Selective Volume Increase in Elevated Extracellular Potassium Conditions Is Mediated by the Na⁺/K⁺ ATPase and Occurs Independently of Aquaporin 4

ASN Neuro
Volume 0: 1–20
© The Author(s) 2020
Article reuse guidelines:
sagepub.com/journals-permissions
DOI: 10.1177/1759091420967152
journals.sagepub.com/home/asn


Erin Walch^{1,2} , Thomas R. Murphy³ , Nicholas Cuvelier^{3,4},
Murad Aldoghmi³, Cristine Morozova^{3,5}, Jordan Donohue^{3,4} ,
Gaby Young^{3,5}, Anuja Samant^{3,5}, Stacy Garcia^{3,5},
Camila Alvarez^{3,5}, Alex Bilas^{3,4}, David Davila³,
Devin K. Binder^{1,2,4}, and Todd A. Fiocco^{2,3,4} 

Abstract

Astrocytes and neurons have been shown to swell across a variety of different conditions, including increases in extracellular potassium concentration ($[K^+]_o$). The mechanisms involved in the coupling of K^+ influx to water movement into cells leading to cell swelling are not well understood and remain controversial. Here, we set out to determine the effects of $[K^+]_o$ on rapid volume responses of hippocampal CA1 pyramidal neurons and stratum radiatum astrocytes using real-time confocal volume imaging. First, we found that elevating $[K^+]_o$ within a physiological range (to 6.5 mM and 10.5 mM from a baseline of 2.5 mM), and even up to pathological levels (26 mM), produced dose-dependent increases in astrocyte volume, with absolutely no effect on neuronal volume. In the absence of compensating for addition of KCl by removal of an equal amount of NaCl, neurons actually shrank in $[K^+]_o$, while astrocytes continued to exhibit rapid volume increases. Astrocyte swelling in $[K^+]_o$ was not dependent on neuronal firing, aquaporin 4, the inwardly rectifying potassium channel Kir 4.1, the sodium bicarbonate cotransporter NBCe1, or the electroneutral cotransporter, sodium-potassium-chloride cotransporter type 1 (NKCC1), but was significantly attenuated in 1 mM barium chloride ($BaCl_2$) and by the Na^+/K^+ ATPase inhibitor ouabain. Effects of 1 mM $BaCl_2$ and ouabain applied together were not additive and, together with reports that $BaCl_2$ can inhibit the NKA at high concentrations, suggests a prominent role for the astrocyte NKA in rapid astrocyte volume increases occurring in $[K^+]_o$. These findings carry important implications for understanding mechanisms of cellular edema, regulation of the brain extracellular space, and brain tissue excitability.

Keywords

cell swelling, cellular edema, extracellular space, Kir4.1, NBCe1, NKCC1, K⁺ buffering, sodium-potassium pump, volume regulation

Received September 21, 2020; Accepted for publication September 23, 2020

¹Division of Biomedical Sciences, School of Medicine, University of California, Riverside, Riverside, United States

²Center for Glial-Neuronal Interactions, University of California, Riverside, Riverside, United States

³Department of Molecular, Cell and Systems Biology, University of California, Riverside, Riverside, United States

⁴Interdepartmental Graduate Program in Neuroscience, University of California, Riverside, Riverside, United States

⁵Undergraduate Major in Neuroscience, University of California, Riverside, Riverside, United States

Corresponding Author:

Todd A. Fiocco, 1109 Biological Sciences Bldg., Department of Molecular, Cell and Systems Biology, University of California, Riverside, Riverside, CA 92521, United States.

Email: toddf@ucr.edu



Astrocytes play a significant role in maintaining ion and neurotransmitter concentrations in the extracellular space (ECS). This includes uptake of glutamate and potassium ions that are released during synaptic transmission. Potassium influx into astrocytes during neuronal synaptic activity is redistributed through the glial syncytium to areas of lower potassium concentration, a process known as “potassium spatial buffering” (Walz, 2000; Kofuji and Newman, 2004). Potassium influx into astrocytes is thought to be coupled to movement of water into the cell, leading to transient or prolonged fluxes in cellular volume (Pasantes-Morales and Schousboe, 1989; Walz, 1992; MacVicar et al., 2002; Risher et al., 2009). Volume changes in astrocytes have been measured in a number of different ways, both directly using fluorescence microscopy (Risher et al., 2009; Benesova et al., 2012) and inferred by recording changes in intracellular ion concentrations (Walz, 1992), light scattering (Andrew and MacVicar, 1994), or assessment of the size or composition of the ECS (Ransom et al., 1985; Traynelis and Dingledine, 1988; Binder et al., 2004; Larsen et al., 2014). While evidence suggests that elevated extracellular potassium leads to astrocyte volume increases, the mechanisms involved have remained controversial.

Astrocytes express an impressive array of potassium channels and cotransporters, including many not expressed by other cell types, which may be responsible for elevated K^+ -induced astrocyte swelling. One such channel both highly expressed and unique to glial cells is Kir4.1, an inwardly rectifying potassium channel that is thought to play a role in the spatial buffering of potassium (Kalsi et al., 2004; Kofuji and Newman, 2004). Interestingly, Kir4.1 has been linked to the astrocyte-specific water channel aquaporin 4 (AQP4; Connors et al., 2004; Nagelhus et al., 2004), providing a means for the coupling of K^+ fluxes to water movement. Another possible candidate is the sodium-potassium-chloride cotransporter type 1, NKCC1. NKCC1 may contribute to potassium-mediated astrocyte swelling in the optic nerve (MacVicar et al., 2002), and it plays a clear role in $[K^+]_o$ -induced astrocyte swelling *in vitro* (Su et al., 2002a). However, its role in intact tissue has been less convincing (Larsen et al., 2014). NKCC1 is especially compelling due to its high purported water permeability (Macaulay and Zeuthen, 2012). Finally, evidence suggests that the $\alpha_2\beta_2$ isoform of the Na^+/K^+ ATPase (NKA), which is highly expressed by astrocytes (Cholet et al., 2002; Stoica et al., 2017; Melone et al., 2019), is most sensitive to changes in extracellular potassium (Larsen et al., 2014), providing a route for K^+ influx into astrocytes that could couple to water movement.

While cellular volume increases have a powerful influence on neuronal and brain tissue excitability, the precise contribution of astrocyte swelling has not been clearly defined. In $[K^+]_o$ elevated to 8.5 mM, neurons generate

synchronous ictal bursting activity that requires NMDA receptor activation and reduction of the ECS (Traynelis and Dingledine, 1988). In these conditions, although direct cell volume measurements were not taken, it was speculated that the reduction of the ECS was due to astrocyte swelling tied to influx of K^+ (Traynelis et al., 1989). Therefore, astrocyte swelling may directly contribute to neuronal excitability and seizure generation.

The phenomenon of neuronal swelling is a topic of contention among groups studying cellular volume changes. Earlier work in acute slices demonstrated recordable changes in light transmittance (LT) after challenging slices with known triggers of tissue swelling—hypoosmolar and $[K^+]_o$ artificial cerebrospinal fluid (ACSF; Andrew and MacVicar, 1994). LT was said to positively correlate with swelling, although the authors did notice a relationship between neuronal activity and LT. With the advent of 2-photon laser microscopy (2PLSM), volume changes at the single-cell level could be estimated (Davies et al., 2007). Combining traditional LT and tissue resistance techniques with newly devised methods of 2PLSM image analysis, neurons were reported to swell under conditions of oxygen-glucose deprivation and $[K^+]_o$, but not hypoosmolarity (Andrew et al., 2007). In another 2PLSM study (Rungta et al., 2015), neuronal swelling was observed after electrical stimulation intending to mimic the excitotoxicity that triggers primary Na^+ influx and later Cl^- influx. Induction of spreading depression (SD) via localized elevations in $[K^+]_o$ leads to apparent dendritic beading when visualized with 2PLSM (Steffensen et al., 2015; Sword et al., 2017). Interestingly, our past work recording cellular volume changes indicated that neurons do in fact swell under hypoosmolar conditions (Murphy et al., 2017). However, comparison of neuronal versus astrocyte volume in varying concentrations of $[K^+]_o$ in a pathophysiological range has not been performed previously.

In this study, we set out to determine the effects of $[K^+]_o$ on volume of CA1 pyramidal cells and astrocytes in stratum radiatum using real-time confocal volume measurements of fluorescently labeled cells in acute hippocampal slices. Slices were exposed to standard ACSF, as well as $[K^+]_o$ ACSF at concentrations of 6.5, 10.5, or 26 mM. Two different conditions of $[K^+]_o$ were used, one in which addition of KCl was compensated for by removal of an equal amount of NaCl to maintain extracellular osmolarity, and the other in which only KCl was added without changing NaCl concentration. In both conditions, astrocytes dose-dependently increased their volume, while neurons either steadfastly maintained their volume or actually shrank significantly due to the increased extracellular osmolarity by addition of $[K^+]_o$. Even at 26 mM $[K^+]_o$, neurons completely resisted volume change, suggesting an inability to remove excess extracellular K^+ . Astrocyte volume increases in $[K^+]_o$

were not due to AQP4, Kir4.1, electrogenic sodium bicarbonate cotransporter 1 (NBCe1), NKCC1, or neuronal action potential generation but were reduced significantly in 1 mM barium chloride (BaCl₂) and by the NKA inhibitor ouabain. Our findings are consistent with previous studies citing the importance of the Na⁺/K⁺ pump on astrocyte volume increases associated with influx of K⁺ (Larsen et al., 2014).

Materials and Methods

All experiments were performed in accordance with National Institutes of Health guidelines for the care and use of laboratory animals and approved by the Institutional Animal Care and Use Committee at the University of California, Riverside.

Slice Preparation

Hippocampal slices were prepared from C57Bl/6J mice or transgenic mice on the C57Bl6 background at 15 to 21 days of age as described previously (Xie et al., 2014). In some astrocyte imaging experiments, use of hippocampal slices from *mGFAP-Cre;Rosa26^{lsl-tdTomato}* transgenic mice replaced C57Bl/6J mice. For experiments requiring neuronal imaging, Thy1-GFP-S or Thy1-GFP-M transgenic mice were used instead (#011070 and 007788, respectively; Jackson Laboratories, Bar Harbor, ME, USA). These mice have been repeatedly backcrossed to a C57Bl/6J background and exhibit no obvious differences in phenotype compared with wild-type mice (Feng et al., 2000). Animals were anesthetized under isoflurane and rapidly decapitated, and brains were removed quickly into petri dishes containing oxygenated (Carbogen, 95% oxygen and 5% carbon dioxide), ice-cold slicing buffer. Standard slicing buffer contained (in mM) the following: 125 NaCl, 2.5 KCl, 3.8 MgCl₂, 1.25 NaH₂PO₄, 26 NaHCO₃, 25 glucose, and 1.3 ascorbic acid. Parasagittal slices (350 μm thick) were cut using an automated vibrating blade microtome (VT1200S model; Leica Biosystems, Buffalo Grove, IL, USA) and transferred to a recovery chamber containing 36°C ACSF solution comprising (in mM) the following: 125 NaCl, 2.5 KCl, 2.5 CaCl₂, 1.3 MgCl₂, 1.25 NaH₂PO₄, 26 NaHCO₃, and 15 glucose. Slices were incubated for 45 min at 36°C, followed by a 15-min recovery period at room temperature, before being used in experiments. In later experiments, the aforementioned protocol was modified slightly to improve slice recovery. Standard slicing buffer was substituted by a sucrose-based slicing buffer containing (mM) the following: 87 NaCl, 75 sucrose, 10 glucose, 1.25 NaH₂PO₄, 2.5 KCl, 25 NaHCO₃, 1.3 ascorbic acid, 0.5 CaCl₂, 7 MgCl₂, 2 pyruvate, 3.5 MOPS, and 0.1 kynurenic acid. Sucrose slicing buffer was used in both slice preparation (as a partially

frozen slush) and in the slice recovery chamber during incubation. After incubation and subsequent cooling to room temperature, slices were transferred to a second chamber containing normal ACSF and allowed to equilibrate for at least 15 min before use in experiments.

The transgenic *mGFAP-Cre;Rosa26^{lsl-tdTomato}* mice express fluorescent tdTomato protein in astrocytes, which allows for imaging of astrocytes in hippocampal slices without exogenous fluorochromes. For astrocyte imaging in C57Bl/6J mice, astrocytes were incubated with sulforhodamine-101 (SR-101; Sigma-Aldrich, St. Louis, MO, USA) as described previously (Schnell et al., 2015; Murphy et al., 2017). In this case, slices were incubated in 1 μM SR-101 and a modified ACSF consisting of (in mM) the following: 1.3 ascorbic acid, 125 NaCl, 15 glucose, 1.25 H₂PO₄, 2.5 KCl, 26 NaHCO₃, 0.5 CaCl₂, and 6 MgCl₂. After incubation (35–45 min at 36°C), slices were transferred to a chamber containing modified ACSF without SR-101 and incubated for an additional 10 min at 36°C. Slices were subsequently transferred to standard ACSF at room temperature for a minimum of 15 min prior to use in experiments. All experiments were then performed at room temperature. Modified ACSF was replaced by sucrose slicing buffer following the protocol modifications described earlier.

Experimental Solutions and Pharmacology

To establish conditions of elevated extracellular potassium, we used 6.5 mM, 10.5 mM, or 26 mM K⁺ ACSF, progressing from a moderate challenge (6.5 mM K⁺), to near ceiling levels reached during seizure (10.5 mM), to a concentration more closely linked to SD models and which has been used in numerous studies previously (26 mM K⁺). Initial $[K^+]_o$ ACSF solutions were kept isoosmolar (~300 mOsm) by equiosmolar omission of NaCl. In a second set of experiments, KCl was elevated with no corresponding change to the NaCl concentration (“nonisoosmolar”) to deliberately examine effects of elevated solution hyperosmolarity by addition of K⁺ on cellular volume changes. The following were the osmolarities of these solutions (in mOsm): 6.5 mM $[K^+]_o$: ~309; 10.5 mM $[K^+]_o$: ~317; 26 mM $[K^+]_o$: ~348. To study the mechanisms of astrocyte swelling in $[K^+]_o$, pharmacologic antagonists were diluted in standard ACSF or isoosmolar 10.5 mM K⁺ ACSF. Drugs were added to the bath at the beginning of the 10-min baseline period prior to the first application of isoosmolar $[K^+]_o$ ACSF and remained in the bath for the entire duration of the experiment. BaCl₂ was used to block Kir4.1 channels at 100 μM (Djukic et al., 2007) and to nonselectively inhibit $[K^+]_o$ channels at 1 mM (Benham et al., 1985; Miller et al., 1987). Disodium 4,4'-diisothiocyanatostilbene-2,2'-disulfonate (DIDS) was applied at a

concentration of 300 μM , which is known to block the sodium bicarbonate transporter (Lu and Boron, 2007; Larsen and MacAulay, 2017). Bumetanide is a widely used diuretic and was applied at 10 μM to block the sodium-potassium-chloride cotransporter NKCC1 (Larsen et al., 2014). Complete block of the astrocyte sodium-potassium ATPase was achieved by applying 50 μM ouabain (Larsen et al., 2014). Higher ouabain concentrations are required to fully block the neuronal Na^+/K^+ pump isoform, but ouabain at high concentration can lead to slice health deterioration as reported by others (Larsen et al., 2014). In one experiment, tetrodotoxin (TTX) was administered to slices at 1 μM to block voltage-gated sodium channels and thus prevent the generation of action potentials.

Electrophysiology

Following recovery, slices were transferred to a recording chamber and continuously perfused with oxygenated ACSF at room temperature. Slices and individual CA1 pyramidal cells were visualized on a Leica DLMFSA upright microscope, with HCX APO L20x/0.50W U-V-I and HCX APO L63x/0.90W U-V-I submersion objectives and differential interference contrast optics (Leica Microsystems, Buffalo Grove, IL, USA). Whole-cell patch clamp recordings were acquired using a Multiclamp 700B amplifier and Digidata 1550 digitizer, controlled using pClamp v.10.7.0.3 and Multiclamp Commander v.2.2.2.2 software (Molecular Devices, Sunnyvale, CA, USA). Patch pipettes were pulled from thin-wall 1.5 mM borosilicate glass capillaries World Precision Instruments using a Narishige PC-10 vertical micropipette puller (Narishige, Tokyo, Japan). Patch pipette resistances ranged from ~ 3 to 5 mOhm when filled with an internal solution containing the following (in mM): 140 K-gluconate, 4 MgCl_2 , 0.4 ethylene glycol-bis(β -aminoethyl ether)-N,N,N',N'-tetraacetic acid (EGTA), 4 Mg-ATP, 0.2 Na-GTP, 10 2-[4-(2-hydroxyethyl)piperazin-1-yl]ethanesulfonic acid (HEPES), and 10 phosphocreatine, pH 7.3 with KOH. CA1 pyramidal neurons were identified using differential interference contrast optics based on their location in stratum pyramidale and their characteristic morphology including apical dendrites arborizing into the hippocampal molecular layer. Upon attaining the whole-cell configuration, the cell resting V_m and R_m were recorded, and a voltage-step protocol was run to verify the presence of voltage-gated sodium and potassium currents. The cell was then placed into current "I=0" mode to continuously record membrane potential. After a 10-min baseline recording, 10.5 mM $[\text{K}^+]_o$ isoosmolar ACSF was applied to measure effects on V_m and action potential generation, followed by a 10-min wash period in control ACSF. Only a single neuronal current clamp recording was made per slice.

Imaging

Throughout our experiments, enhanced green fluorescent protein (eGFP) was excited using a 488-nm argon laser and detected with a 503–548 nm bandpass filter, and SR-101 was excited with a 559-nm semiconductor laser and detected with a 624–724 nm bandpass filter using an Olympus Fluoview FV1000 (FV10-ASW) confocal imaging system. The objective used was an Olympus LUMPlanFI 60x/0.90 W $\infty/0$ water immersion objective lens. Confocal laser settings were the same as described previously (Murphy et al., 2017). Output power for both lines was kept as low as possible (1.5%) to minimize the possibility for light-induced artifacts. Volume imaging of neurons and astrocytes was performed as described previously (Murphy et al., 2017). Briefly, z-stacks of 1- μm -thick images were collected at 1-min intervals over individual cell somata within 15 s to ensure adequate coverage of the soma and main processes while at the same time preventing data loss caused by tissue volume changes. Stacks were collected using a 2–3.5 \times zoom factor, with a scan area clipped close around the soma to increase imaging speed. Cell drift in the x-y-z planes was compensated using quick X-Y scans and X-Y-Z adjustments as necessary between time points. Briefly, imaging experiments consisted of three steps: (1) A 5- to 10-min baseline period in standard ACSF, in which 2 to 3 z-stacks were acquired in succession at 1-min intervals and averaged to serve as the baseline comparison for later time points; (2) a 5-min application of $[\text{K}^+]_o$ ACSF, during which z-stacks through the full thickness of the cell were collected each minute; and (3) a 10-min wash period in standard ACSF, during which an image was taken every 5 min. Steps (2) and (3) were then repeated once each, after which the slice was discarded. Fiji/Image J was used for thresholding of image stacks and subsequent volume analysis as previously described (Murphy et al., 2017). Area of compressed image stacks (used as a proxy for cell volume) was analyzed with cell volume changes reported as percent change from the averaged baseline.

Statistical Analysis

Statistical analysis was carried out using SPSS Statistics 24 software and Laerd Statistics methodology. For analysis of volume measurements, a two-way mixed analysis of variance (ANOVA) was used to check for significant interactions between the within-subject (time) and between-subjects (group/condition) factors. If a significant interaction was noted, a one-way ANOVA was conducted for the between-subjects factors, and a one-way repeated-measures ANOVA was used for the within-subjects factors. In cases where there was a significant interaction between time and condition, a subsequent

independent Student's *t* test (two groups) or one way ANOVA (three groups) was performed. Repeated-measures ANOVA was used for all conditions of cell swelling, comparing two or more treatment groups. "Extreme" values in SPSS boxplots, and/or studentized residuals larger than ± 2.5 following a repeated-measures ANOVA, were used as indicators of potential outliers. Outliers were removed only in cases where there were severe violations of normality or homogeneity, which were improved upon removal of that instance. Violations of normality were identified with the Shapiro–Wilk test, while homogeneity of variance was assessed with Levene's test for equality of variance. Box's test established equality of covariances, and Mauchly's test determined sphericity of the data set. The Greenhouse–Geisser estimation was used to determine significance in the two-way mixed ANOVA. At time points where the condition of normality was violated, nonparametric tests (Kruskal–Wallis or Mann–Whitney U) were used to determine significance. At time points with homogeneity of variance violations, an unequal variance *t* test (Welch's test) was used to check for significance. After one-way ANOVA, post hoc testing (Tukey or Games–Howell) was performed in data sets with two or more groups. For repeated-measures ANOVA run for two or more comparisons, post hoc testing (Holm–Bonferroni) accounted for the type-I error associated with multiple comparisons. Electrophysiology data were analyzed using a nonparametric one-way ANOVA (aka Kruskal–Wallis H test). The distribution of values across treatment groups was not similar upon inspection of boxplots. Accordingly, pairwise comparisons using Dunn's procedure were performed with Bonferroni correction for multiple comparisons. For all experiments, each group contained $N=8$ – 12 cells (numbers specified in each experiment), unless otherwise noted. Significance values are listed as follows: $*p < .05$, $**p < .01$, and $***p < .001$.

Results

$^{+}[K]_o$ ACSF Selectively Swells Astrocytes

We first recorded cellular volume of both CA1 pyramidal neurons and astrocytes within the stratum radiatum in response to 6.5, 10.5, and 26 mM $[K^+]_o$ ACSF. This ACSF was made isoosmolar by removal of NaCl (see Materials and Methods section). Astrocytes were labeled with either SR-101 (Schnell et al., 2015) or by expression of TdTomato driven by the *mGFAP* promoter (*mGFAP-Cre; Rosa26^{sl-tdTomato}*). Astrocytes were identified by their characteristic bushy morphology with 1–3 main processes emerging from the cell soma, with subsequent branching into many increasingly smaller and finer processes. To image pyramidal neurons, slices were taken from Thyl-

eGFP mice (Feng et al., 2000) where select CA1 neurons express eGFP. These mice express eGFP in a small proportion of CA1 pyramidal neurons, enabling easy visualization of individual cells. Pseudocolor images illustrate the increase in soma area over baseline in astrocytes exposed to $^{+}[K]_o$ (magenta outline in image overlays; Figure 1A to C), as well as the persistent soma area in neurons unaffected by $^{+}[K]_o$ (Figure 1D). Application of laser light alone had no effect on cell volume over time for either astrocytes or neurons (Figure 1E). Consistent with the role of astrocytes in potassium clearance, we found that astrocytes rapidly swelled in $^{+}[K]_o$ (within 1 min), whereas there was little to no change in neurons (Figure 1F to H). Astrocyte volume reached a maximum of 4.3% above baseline at 6.5 mM $[K^+]_o$, 6.6% at 10.5 mM $[K^+]_o$, and 15% at 26 mM $[K^+]_o$ after 5 min (the maximum $^{+}[K]_o$ exposure time) during the first application. Similar values were attained in the same astrocytes during a second application of $^{+}[K]_o$ after an intervening 10-min wash period during which astrocytes recovered to baseline volume. Even in 6.5 mM $[K^+]_o$ ACSF, within 1 min there was a significant increase in astrocyte volume in comparison to neurons which remained at or very near baseline (Figure 1F, $**p < .01$). Neuronal volume remained unchanged even in 26 mM $[K^+]_o$, which is far above the estimated ceiling levels of K^+ during seizure (10–15 mM) but which may be reached during energy failure in conditions of stroke. The resilience of neurons to volume change in 26 mM $[K^+]_o$ is somewhat surprising, as similar levels of $[K^+]_o$ have been shown to swell neurons in previous studies (Andrew et al., 2007; Zhou et al., 2010; Tang et al., 2014). We attribute the lack of neuronal swelling to the absence of SD in our conditions. Without the occurrence of SD, the elevated $[K^+]_o$ alone appears to swell astrocytes specifically, consistent with their role in K^+ homeostasis. To ensure that these CA1 neurons are capable of swelling, we performed experiments in which application of 10.5 mM $[K^+]_o$ was followed by application of 40% hypoosmolar ACSF. In line with our previous findings (Murphy et al., 2017), neurons rapidly swelled in hypoosmolar conditions, despite their resistance to volume change in $^{+}[K]_o$ (Figure 1I).

Increased ACSF Osmolarity due to Addition of $[K^+]_o$ Attenuates Astrocyte Swelling and Leads to Neuronal Shrinking

Because elevations in $[K^+]_o$ would not normally be associated with an equiosmolar decrease in $[Na^+]_o$, we next assessed astrocyte and neuronal volume in $^{+}[K]_o$ solution without compensating by removal of NaCl. In these conditions, addition of K^+ to the ACSF increases the solution osmolarity relative to the control solution (see Materials and Methods section). The elevated

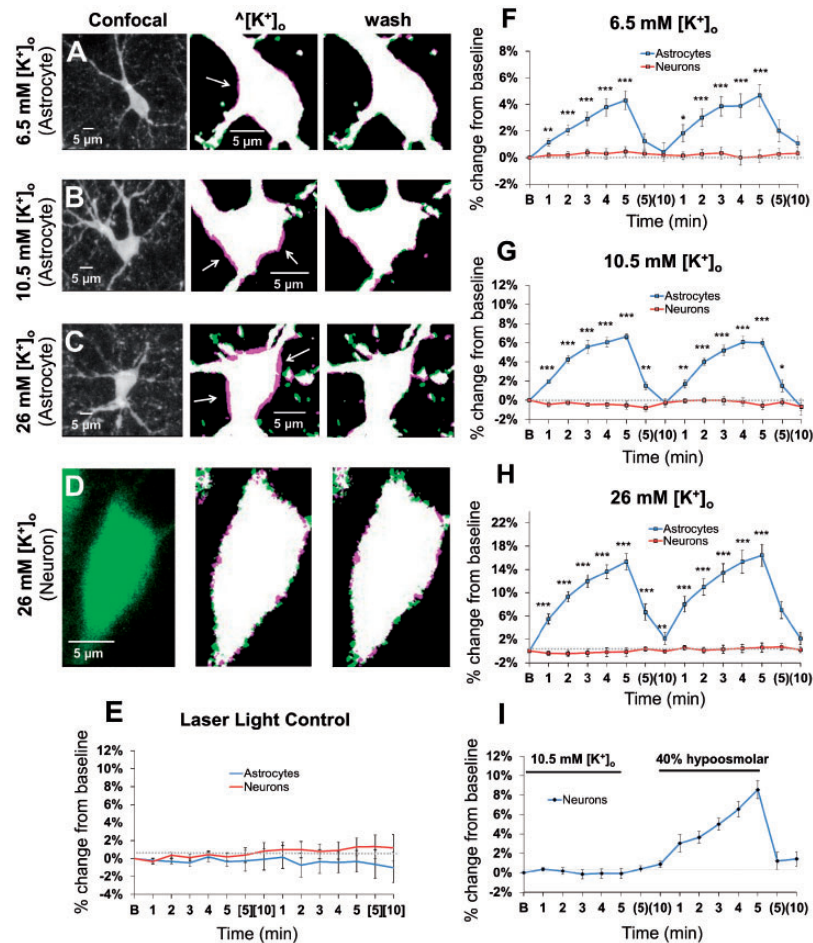


Figure 1. Elevated $[K^+]_o$ ACSF Selectively Swells Astrocytes. $[K^+]_o$ was raised from a baseline of 2.5 mM in control ACSF by addition of KCl, with removal of an equal amount of NaCl to preserve solution osmolarity (see Materials and Methods section). (A–D) Representative confocal images of stratum radiatum astrocytes (A–C) and a CA1 pyramidal neuron (D) in control ACSF show general cell morphology (left panels). Middle panels in (A–D) show thresholded, pseudocolor images of the same cells taken after 5 min in $\Delta[K^+]_o$ at 6.5 mM (A), 10.5 mM (B) or 26 mM (C, D), overlaid onto the baseline image. Increase in cell volume in the image overlays is indicated by a magenta outline (white arrows). “Wash” is the image taken after the first 10-min wash period overlaid onto the baseline image (right panels) to show recovery of cell volume in control ACSF. (E) Application of laser light alone to acute slices perfused with control ACSF for the duration of an imaging experiment (20 min) had no effect ($\pm \sim 1\%$) on the volume of astrocytes ($n=6$) or neurons ($n=6$). (F) 6.5 mM $[K^+]_o$ increased the volume of astrocytes in a time-dependent manner, to approximately 4.3% to 4.6% above baseline after 5 min. Return to control ACSF (time points (5) and (10)) led to recovery of cell volume to near baseline. Neurons exposed to 6.5 mM $[K^+]_o$ did not undergo changes in volume ($n=7$). At all time points tested, astrocyte volume was significantly greater than neuronal volume, which remained at or near baseline ($*p < .05$, $**p < .01$, or $***p < .001$; $n=9$ astrocytes, 7 neurons). (G) Application of 10.5 mM $[K^+]_o$ triggered astrocyte volume increase to $\sim 6\%$ above baseline, significantly greater than neuronal volume at all time points, which remained within 1% of baseline ($*p < .01$ or $***p < .001$; $n=9$ astrocytes, 7 neurons). (H) 26 mM $\Delta[K^+]_o$ increased astrocyte volume by up to 15%, significantly greater than neuronal volume at all time points ($***p < .001$; $n=8$ astrocytes, 10 neurons). (I) Dose-response of astrocyte and neuronal volume at the 5 min time point of the first application of $\Delta[K^+]_o$. At each concentration, astrocyte volume was significantly greater than neurons, which steadfastly maintained their volume in elevated $\Delta[K^+]_o$. ($***p < .001$).

extracellular osmolarity is predicted to shrink cells, offsetting K^+ -induced volume increases. We refer to these conditions as “nonisoosmolar” to distinguish from the isoosmolar $\Delta[K^+]_o$ conditions used initially. Nonisoosmolar $\Delta[K^+]_o$ still resulted in clear expansion of the astrocyte soma over baseline (Figure 2A and B). Neurons, however, did not exhibit any obvious change in volume relative to baseline in 10.5 mM $[K^+]_o$ (Figure 2C),

but cell shrinking was visibly apparent after 5 min in 26 mM $[K^+]_o$ (Figure 2D). Although somewhat blunted compared with astrocyte volume increases in isoosmolar $\Delta[K^+]_o$, there were still significant increases in astrocyte volume over baseline at all concentrations of $\Delta[K^+]_o$ tested (Figure 2E to G). Neurons actually exhibited significant shrinking at each $[K^+]_o$ in a dose- and time-dependent manner, with highly significant differences

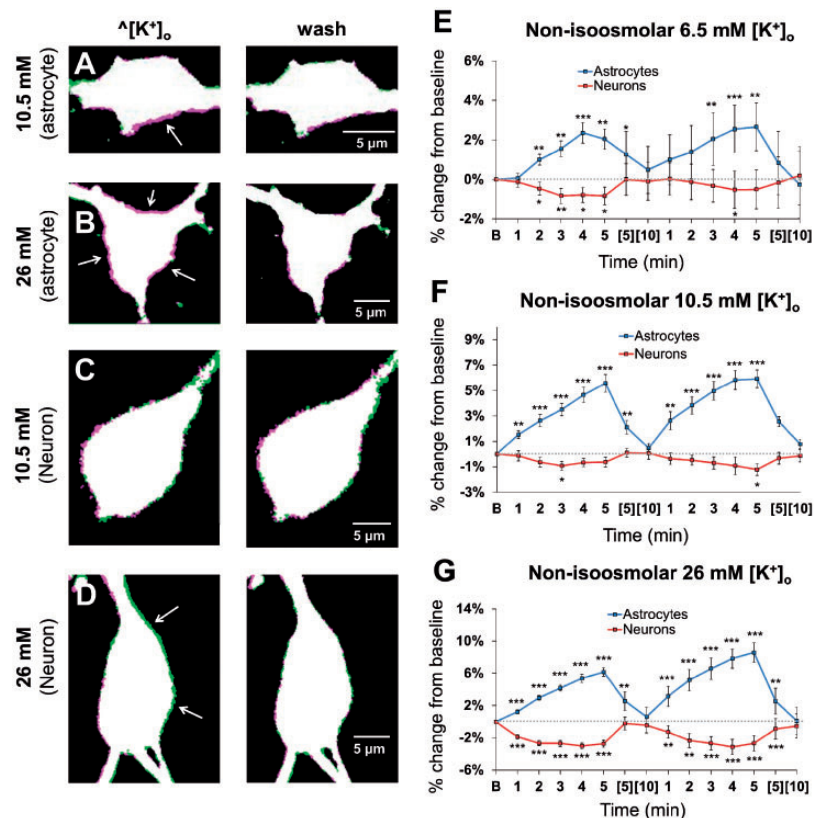


Figure 2. Increased Solution Osmolarity by Addition of K^+ Attenuates Astrocyte Swelling and Shrinks Neurons. KCl was added to control ACSF to elevate $[K^+]_o$ from 2.5 mM without a corresponding removal of NaCl. The resulting “nonisoosmolar” $\wedge[K^+]_o$ was applied over 5 min followed by a 10 min “wash” in control ACSF. (A–D) Representative thresholded images of astrocytes (A, B) and neurons (C, D) after 5 min in $\wedge[K^+]_o$ overlaid onto the baseline image to show volume changes (left panels). The magenta outline reveals volume expansion, while green indicates cell shrinking. Astrocytes in 10.5 mM (A) and 26 mM (B) nonisoosmolar $[K^+]_o$ swell, while neuronal shrinking is visibly apparent at 26 mM $[K^+]_o$ but not at 10 mM $[K^+]_o$ after 5 min (C, D). Any changes in cell volume recover to baseline during the “wash” period (right panels). (E) Dose-response of cell volume illustrates the peak volume change of both cell types after 5 min in nonisoosmolar $\wedge[K^+]_o$. Dampening of astrocyte swelling and neuronal shrinking are most evident at the 26 mM $[K^+]_o$ dose. (F–H) Summary data of astrocyte and neuron volume changes at the different nonisoosmolar concentrations of $[K^+]_o$ relative to baseline volume. Astrocyte volume increased significantly over baseline at 6.5 mM $[K^+]_o$ ($n = 11$) (F), 10.5 mM $[K^+]_o$ ($n = 8$) (G), and 26 mM $[K^+]_o$ ($n = 9$). Neurons, however, exhibited significant shrinking in a dose- and time-dependent manner (6.5 mM $[K^+]_o$, $n = 9$; 10.5 mM $[K^+]_o$, $n = 10$; 26 mM $[K^+]_o$, $n = 9$) and recovered to baseline volume after 10 min in control ACSF ($\wedge[K^+]_o$ wash). Significance is indicated as percent change from baseline within cell at $*p < .05$, $**p < .01$, or $***p < .001$.

occurring at 26 mM $\wedge[K^+]_o$ (Figure 2E to G). These results reaffirm the key role astrocytes play in sequestering elevated $[K^+]_o$.

We next directly compared astrocyte and neuron volume in isoosmolar versus nonisoosmolar $\wedge[K^+]_o$ to determine the effect of osmolarity on cell volume in $\wedge[K^+]_o$ (Figure 3). The increase in osmolarity of 6.5 mM $\wedge[K^+]_o$ led to an insignificant but noticeable decrease in the swelling of astrocytes, in comparison to swelling evoked in isoosmolar 6.5 mM $\wedge[K^+]_o$ (Figure 3A). Neurons did not change their volume in isoosmolar 6.5 mM $\wedge[K^+]_o$, although there was a small but insignificant shrinking of neurons in nonisoosmolar 6.5 mM $\wedge[K^+]_o$ (Figure 3A). In the first application of nonisoosmolar 10.5 mM $\wedge[K^+]_o$, astrocytes swelled significantly

less at minutes 2 and 3 in comparison to isoosmolar 10.5 mM $\wedge[K^+]_o$ (Figure 3B). Neurons maintained their original volume, regardless of the osmolarity of 10.5 mM $\wedge[K^+]_o$ (Figure 3B). In the second application of nonisoosmolar 10.5 mM $\wedge[K^+]_o$, there were insignificant and nearly imperceptible changes in astrocyte swelling and neuron volume compared with those in isoosmolar 10.5 mM $\wedge[K^+]_o$ (Figure 3B). Astrocyte swelling was significantly lower in nonisoosmolar compared with isoosmolar 26 mM $\wedge[K^+]_o$ (Figure 3C and D), likely due to hyperosmolarity-induced shrinking mitigating volume increases associated with K^+ influx. Surprisingly, neuronal shrinking in 26 mM nonisoosmolar $\wedge[K^+]_o$ was significant compared with isoosmolar 26 mM $[K^+]_o$ (Figure 3C and E). Neuronal shrinking and reduced

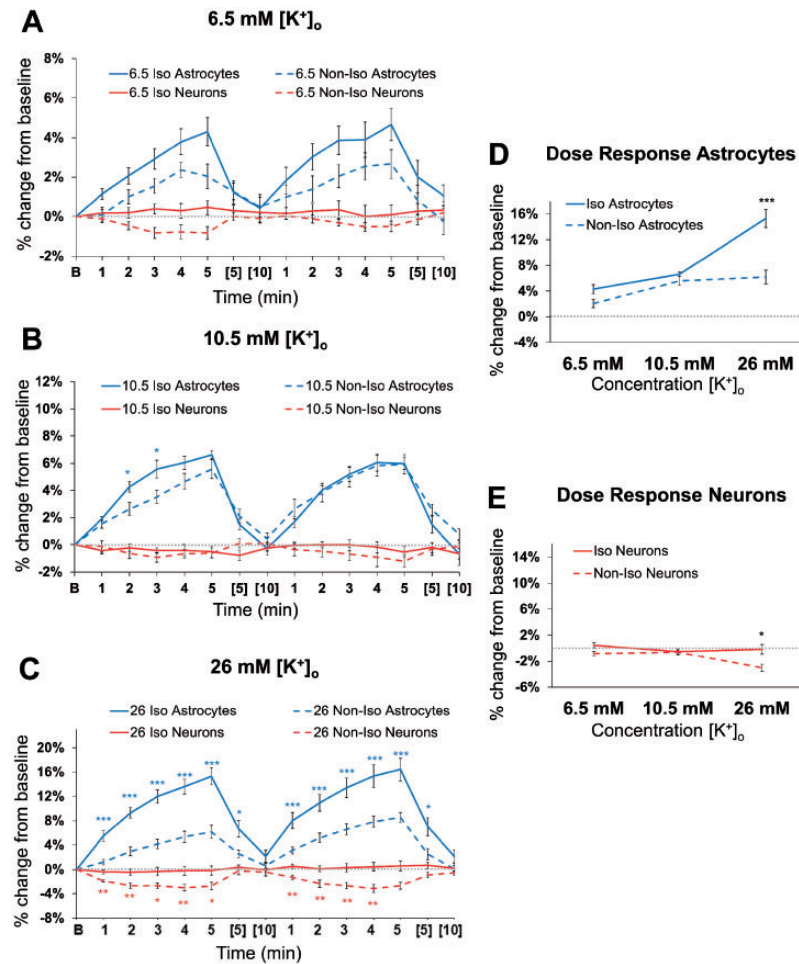


Figure 3. Comparison of Astrocyte and Neuron Volume in Isoosmolar Versus Nonisoosmolar $^{[K^+]_o}$. Data from Figures 1 and 2 have been reassembled to highlight effects of increased extracellular osmolarity on cell volume in $^{[K^+]_o}$. At each concentration of $^{[K^+]_o}$, cell types are specified by color (astrocytes blue, neurons red), and the ACSF osmolarity indicated by dotted (nonisoosmolar) or solid (isoosmolar) lines. Blue asterisks indicate significant differences between astrocyte volume across osmolarity treatments, with red asterisks indicating the same for neurons. (A) Although the effect of the increased osmolarity by addition of K^+ is readily apparent in reducing the volume of cells, the osmolarity of 6.5 mM $^{[K^+]_o}$ treatment did not have a significant effect on the swelling of astrocytes or shrinkage of neurons. (B) At 10.5 mM $^{[K^+]_o}$, the increase in osmolarity led to a small but significant reduction in astrocyte swelling at minutes 2 and 3 ($*p < .05$) during $^{[K^+]_o}$ exposure. During the second 10.5 mM $^{[K^+]_o}$ application, there was no difference in the swelling of astrocytes across treatments. Similarly, the osmolarity of 10.5 mM $^{[K^+]_o}$ application had no significant effect on the volume of neurons. (C) Nonisoosmolar 26 mM $^{[K^+]_o}$ ACSF significantly decreased astrocyte swelling ($***p < .001$) and significantly shrank neurons ($*p < .05$ or $**p < .01$) compared with isoosmolar treatment. (D) Dose-response of iso- versus nonisoosmolar $^{[K^+]_o}$ treatment in astrocytes shows minimal effect of osmolarity on astrocyte $^{[K^+]_o}$ -induced volume increases, except at the highest dose where the increase in osmolarity by 26 mM $^{[K^+]_o}$ significantly dampened the volume change ($***p < .001$). (E) Overall, effects of $^{[K^+]_o}$ and extracellular osmolarity on neuron volume are negligible at 6.5 and 10.5 mM. Only at 26 mM $^{[K^+]_o}$ does the osmolarity increase trigger significant ($\sim 3\%$) shrinkage of neurons from baseline volume.

astrocyte swelling in nonisoosmolar $^{[K^+]_o}$ suggested some amount of outward water movement due to solution hyperosmolarity.

Hyperosmolar ACSF by Addition of Mannitol Shrinks Both Neurons and Astrocytes

To verify that neurons and astrocytes are capable of shrinking in hyperosmolar solution, we raised the

osmolarity of the ACSF by addition of mannitol. This manipulation has the advantage of altering solution osmolarity without changing extracellular ion concentrations. Application of 40% hyperosmolar ACSF by addition of mannitol shrank both astrocytes and neurons (Figure 4), although astrocytes shrank significantly more than neurons during the second + mannitol application (Figure 4C, $*p < .05$, $**p < .01$ or $***p < .001$). These findings suggest, together with our previous work

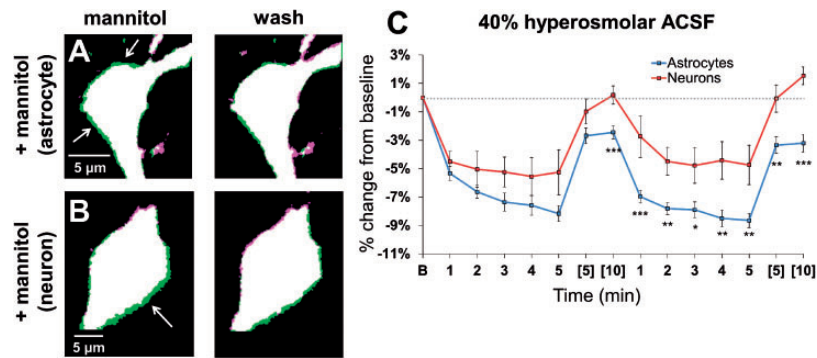


Figure 4. Hyperosmolar ACSF Shrinks Both Neurons and Astrocytes. Pseudocolor images of an astrocyte (A) and neuron (B) at baseline overlaid with the image taken after 5 min in mannitol-supplemented ACSF (“mannitol”; left) and then after return to control ACSF for 10 min (“wash”). Green coloring (white arrows) indicates reduction in soma volume compared with the baseline image. (C) Application of 40% hyperosmolar ACSF (by addition of mannitol) led to shrinking of both astrocytes ($n = 14$) and neurons ($n = 10$) during both 5 min application periods. Upon return to control ACSF, neurons completely recovered their volume, while astrocytes remained at most 3.3% below baseline volume. Astrocyte shrinking was significantly greater than neurons at all time points during and after the second application of hyperosmolar ACSF (* $p < .05$, ** $p < .01$ or *** $p < .001$). ACSF = artificial cerebrospinal fluid.

(Murphy et al., 2017) and data in Figure 1I, that neurons readily respond to changes in solution osmolarity with swelling or shrinking but resist volume change in response to changes in $[K^+]_o$. Our data also support the idea that reduced astrocyte swelling and neuronal shrinking in nonisoosmolar $[K^+]_o$ ACSF is due to the increased osmolarity by addition of K^+ rather than possible alterations in volume regulatory mechanisms through changes in extracellular ion concentrations.

The Cotransporter NKCC1 and the Sodium Bicarbonate Cotransporter NBCe1 Are Not Responsible for Astrocyte Swelling in $[K^+]_o$

We next considered the possibility that influx of bicarbonate ions induced by astrocyte depolarization (Larsen and MacAulay, 2017) could be responsible for astrocyte swelling in $[K^+]_o$ ACSF, as this has previously been demonstrated in astrocytes (Florence et al., 2012). To determine the contribution of the sodium bicarbonate cotransporter NBCe1, we used DIDS (300 μ M) as an antagonist (Larsen and MacAulay, 2017). We observed no appreciable effect of DIDS on astrocyte swelling (Figure 5A and E).

Previous work suggests that the electroneutral ion cotransporter NKCC1 is a key in K^+ influx pathway coupled to cellular volume changes (Mongin et al., 1994; MacVicar et al., 2002; Su et al., 2002a, 2002b; Jayakumar and Norenberg, 2010). NKCC1 is especially intriguing not only because of its role as an ion cotransporter but also because it has been shown to exhibit water permeability (Macaulay and Zeuthen, 2012). Therefore, we probed the possible contribution of NKCC1 to astrocyte swelling in $[K^+]_o$ using the

NKCC1 inhibitor bumetanide. Bumetanide (10 μ M) had no effect on astrocytic swelling in $[K^+]_o$ ACSF (Figure 5B and E), arguing against a role for NKCC1 in astrocyte swelling in our conditions. However, it is worth noting that under hypotonic conditions, cultured astrocytes activate NKCC1 latently (approx. 5–7 min) after exposure (Mongin et al., 1994). This might suggest that NKCC1 could contribute to astrocyte swelling beyond the 5-min period used in our experiments.

Astrocyte Swelling in $[K^+]_o$ Is Not due to K^+ Influx via Kir4.1

We next set out to identify mechanism(s) underlying astrocyte swelling in $[K^+]_o$. In these and subsequent experiments, the isoosmolar $[K^+]_o$ protocol was used, which results in more pronounced astrocyte swelling compared with “nonisoosmolar” $[K^+]_o$. The astrocyte-selective, inwardly rectifying K^+ channel Kir4.1 has long been considered a predominant K^+ influx pathway responsible for extracellular K^+ homeostasis (Kofuji and Newman, 2004; Nagelhus et al., 2004; Lichter-Konecki et al., 2008). Kir4.1-mediated inward potassium currents can be readily recorded in astrocytes (Djukic et al., 2007; Devaraju et al., 2013). The prevailing hypothesis is that water follows the osmotic gradient generated by the influx of K^+ ions into the astrocyte via Kir4.1, resulting in cellular volume changes. To determine any contribution of inwardly rectifying potassium channels to K^+ -induced astrocyte swelling, we measured the astrocyte swelling profiles in the presence of 100 μ M $BaCl_2$, a selective Kir channel blocker (Hille, 1978; Rudy, 1988). Surprisingly, astrocyte swelling in $[K^+]_o$ was not affected by application of 100 μ M $BaCl_2$ ($n = 10$; Figure 5C and F), arguing against a role for Kir4.1.

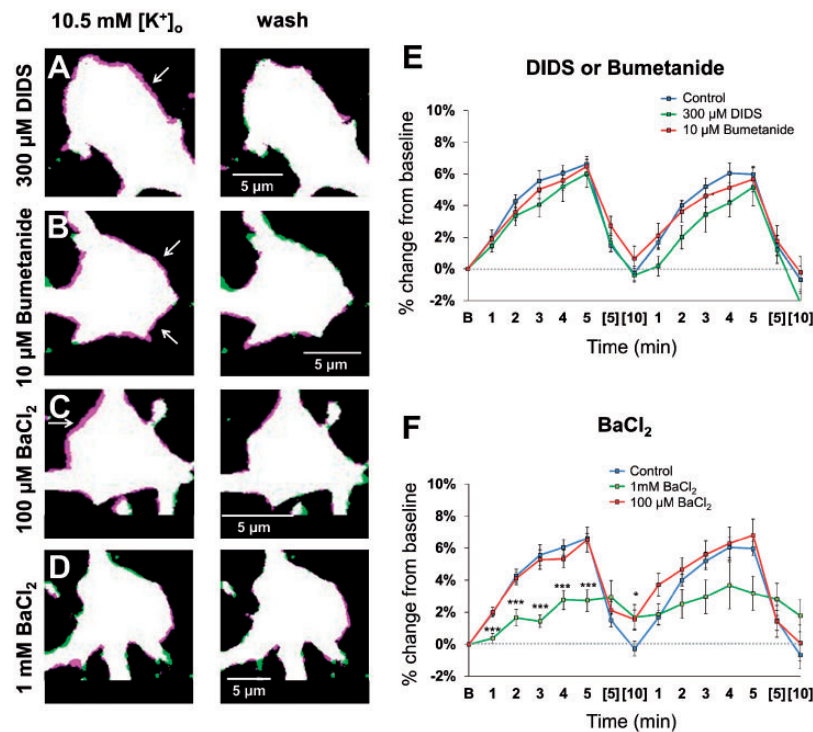


Figure 5. Astrocyte Swelling in $^{10.5}[\text{K}^+]_o$ Is Not due to NBCe1, NKCC1, or Kir4.1. (A–D) Representative astrocyte images taken at 5 min overlaid onto the baseline image in isoosmolar $^{10.5}[\text{K}^+]_o$ in the presence of antagonists for the NBCe1 (DIDS, $300 \mu\text{M}$); NKCC (bumetanide, $10 \mu\text{M}$); Kir4.1 (BaCl_2 , $100 \mu\text{M}$); or K^+ channels in general (BaCl_2 , 1 mM) (left panels) followed by 10-min wash (right panels). Note continued swelling of astrocytes in all conditions except 1 mM BaCl_2 as indicated by the magenta border (white arrows). (E) Summary data showing lack of effect of DIDS ($n = 6$) or bumetanide ($n = 8$) on astrocyte swelling profiles in $^{10.5}[\text{K}^+]_o$ compared with control recordings in the absence of antagonists ($n = 9$). (F) BaCl_2 at $100 \mu\text{M}$ had no effect on astrocyte volume ($n = 10$) but significantly reduced astrocyte volume increases at 1 mM ($n = 8$), suggesting possible involvement of an unidentified K^+ channel. (* $p < .05$, or *** $p < .001$)

DIDS = disodium 4,4'-diisothiocyanatostilbene-2,2'-disulfonate; BaCl_2 = barium chloride.

Barium is also known to nonselectively block K^+ channels at concentrations of 1 mM or more (Benham et al., 1985; Miller et al., 1987). Therefore, to look for a more general role of astrocyte K^+ channels, experiments were performed in 1 mM BaCl_2 (Figure 5D and F). Application of 1 mM BaCl_2 in $^{10.5}[\text{K}^+]_o$ significantly reduced astrocyte swelling to about 2% above baseline, compared with approximately 6% in $^{10.5}[\text{K}^+]_o$ alone. At 1 mM , BaCl_2 is considered to be a nonselective K^+ channel blocker (Walter et al., 2001), preventing identification of the specific K^+ channel(s) that possibly contribute to astrocytic volume increases. However, there is also a literature suggesting that barium at high concentrations nonselectively inhibits the NKA (Walz et al., 1984; Elwej et al., 2017, 2018). This led us to further explore the role of the NKA in $^{10.5}[\text{K}^+]_o$ astrocyte swelling in subsequent experiments.

Astrocyte Swelling in $^{10.5}[\text{K}^+]_o$ Is Significantly Attenuated by the NKA Inhibitor Ouabain

Previous work has reported an important role for the sodium-potassium pump as a K^+ influx pathway in

astrocytes (Walz and Hinks, 1985; Mongin et al., 1994; Larsen et al., 2014, 2016; Stoica et al., 2017). The NKA normally pumps potassium into the cell and sodium outside, against their concentration gradients. It has been shown previously that the astrocyte $\alpha 2/\beta 2$ subunit isoform of the Na^+/K^+ pump is particularly sensitive to changes in extracellular K^+ , which would make it uniquely suited to removing excess extracellular potassium (Larsen et al., 2014; Stoica et al., 2017). Therefore, pumping of K^+ into astrocytes may be associated with the astrocyte volume increases observed in $^{10.5}[\text{K}^+]_o$. To test for a role of the NKA in $^{10.5}[\text{K}^+]_o$ -induced astrocyte swelling, experiments were performed using the NKA inhibitor ouabain. A recent study found ouabain IC₅₀ values of about 1 to $3 \mu\text{M}$ for the $\alpha 2$ isoform expressed in *Xenopus laevis* oocytes, with 200– $300 \mu\text{M}$ for the $\alpha 1$ isoform, which is mainly expressed by neurons (Stoica et al., 2017). We used a concentration of $50 \mu\text{M}$, which is predicted to completely block the astrocyte NKA in brain slices, with partial block of the neuronal isoform (Larsen et al., 2014). In the presence of $50 \mu\text{M}$ ouabain, astrocyte swelling was significantly diminished compared

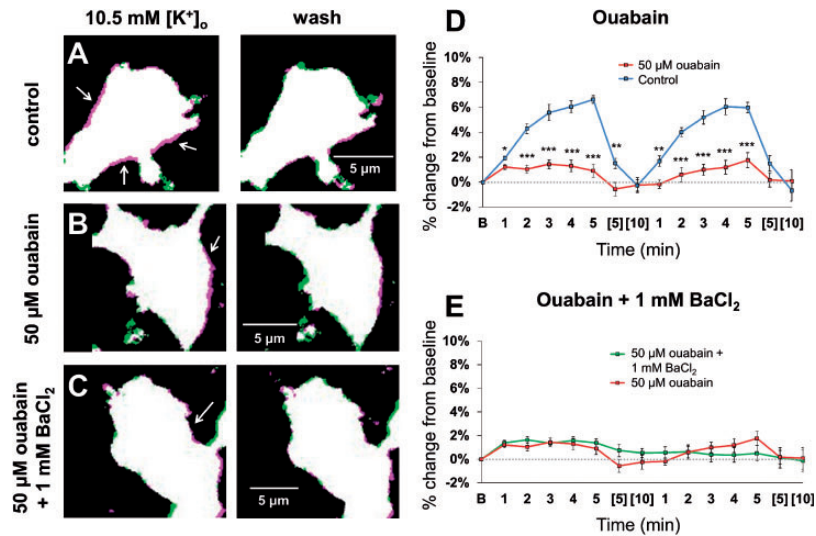


Figure 6. The Na^+/K^+ ATPase Inhibitor Ouabain Significantly Reduces Astrocyte Swelling in $^{\wedge}[\text{K}^+]_o$. (A–C) Representative astrocyte images taken at 5 min in isosmolar $10.5 \text{ mM } [\text{K}^+]_o$ overlaid onto the baseline image for $^{\wedge}[\text{K}^+]_o$ only (A) or $^{\wedge}[\text{K}^+]_o$ in the presence of ouabain ($50 \mu\text{M}$) (B) or ouabain + 1 mM BaCl_2 (C) (left panels). Note the significant reduction in astrocyte swelling in the treatment groups compared with control as indicated by the magenta border around the cells (white arrows). Overlay of the astrocyte image taken after a 10-min wash period in control ACSF with the baseline image shows recovery of volume to baseline (right panels). (C) Ouabain potentially counteracted astrocyte swelling, which led to a significant reduction in astrocyte volume at all time points ($n = 8$; $*p < .05$, $**p < .01$, or $***p < .001$). (D) The combination of $50 \mu\text{M}$ ouabain plus 1 mM BaCl_2 applied together was no different than + ouabain alone ($n = 9$) on suppressing astrocyte swelling in $10.5 \text{ mM } [\text{K}^+]_o$. BaCl_2 = barium chloride.

with control (Figure 6A, B, and D). Next, we reasoned that if the inhibitory effect of 1 mM BaCl_2 on astrocyte swelling was due to block of K^+ channels, then coapplication of 1 mM BaCl_2 plus $50 \mu\text{M}$ ouabain would have an additive effect, reducing astrocyte swelling to near zero. However, there was no additional inhibition of astrocyte swelling in $50 \mu\text{M}$ ouabain + 1 mM BaCl_2 (Figure 6C and E), suggesting that the effect of 1 mM BaCl_2 is likely due to off-target inhibition of the NKA as previously reported (Walz et al., 1984; Elwej et al., 2017, 2018). Similarly, coapplication of $100 \mu\text{M BaCl}_2$ reduced swelling to the same extent as ouabain alone (data not shown). These data suggest that astrocyte swelling in conditions of $^{\wedge}[\text{K}^+]_o$ is predominantly due to K^+ sequestration into astrocytes by the astrocyte NKA, although we cannot completely rule out a possible partial role for unidentified K^+ channels contributing to the astrocyte volume increase.

Astrocyte Swelling in $^{\wedge}[\text{K}^+]_o$ Occurs Independently of the Water Channel AQP4

AQP4 is a functional water channel expressed by astrocytes but not neurons (Nielsen et al., 1997; Nagelhus et al., 1998). In our previous study (Murphy et al., 2017), we found that astrocyte swelling was significantly greater in $\text{AQP4}^{-/-}$ mice in severe hypoosmolar conditions relative to controls, indicating that AQP4 is

dispensable for swelling, and perhaps even important for extrusion of water. However, AQP4 has been shown to colocalize with Kir4.1, lending support to findings suggesting functional coupling of K^+ movement to AQP4-dependent water influx (Nagelhus et al., 1999; Wen et al., 1999; Nagelhus et al., 2004). Therefore, we performed experiments in hippocampal slices from $\text{AQP4}^{-/-}$ and control mice to assess any possible contribution of AQP4 to the water influx associated with astrocyte swelling in $^{\wedge}[\text{K}^+]_o$. Surprisingly, we found an equal amount of swelling in $\text{AQP4}^{-/-}$ astrocytes compared with wild type during the first application of 10.5 mM K^+ (Figure 7A to C). $\text{AQP4}^{-/-}$ astrocytes then did not fully recover to baseline volume during the 10-min wash period in normal ACSF, resulting in significantly higher peak swelling during the second $^{\wedge}[\text{K}^+]_o$ application (Figure 7C). These observations provide additional evidence that AQP4 may play an important role in water efflux to limit astrocyte swelling rather than serve as a required water entry pathway.

Block of Neuronal Firing Does Not Affect Astrocyte Swelling in $^{\wedge}[\text{K}^+]_o$

Raised extracellular K^+ depolarizes neurons and significantly increases neuronal action potential generation (Xie et al., 2012). It is possible that significant increases in neuronal firing could stimulate astrocytic receptors

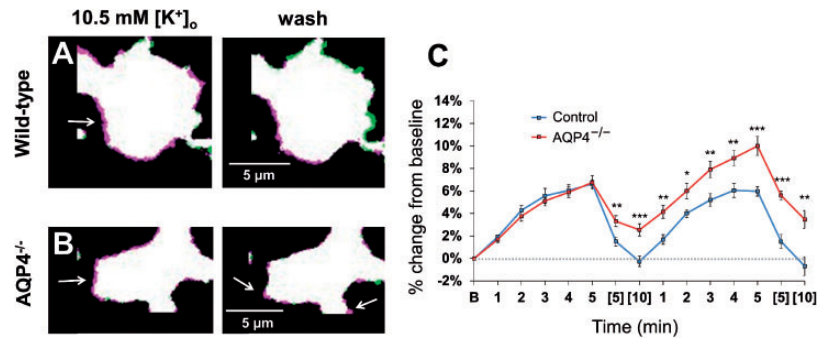


Figure 7. Astrocyte Swelling in $[K^+]_o$ Occurs Independently of the Water Channel AQP4. (A, B) The left panel shows a representative astrocyte image taken after 5 min in isoosmolar 10.5 mM $[K^+]_o$ ACSF overlaid onto the baseline image for (A) wild type and (B) AQP4 $^{-/-}$. On the right is the 10-min wash image relative to baseline to show cell volume recovery. The magenta outline (white arrows) indicates volume expansion over baseline. (C) Wild-type ($n = 9$) and AQP4 $^{-/-}$ ($n = 8$) astrocytes swelled at the same rate and to the same volume during the first exposure to $[K^+]_o$. Note that AQP4 $^{-/-}$ astrocytes failed to return to initial baseline volume after the 10-min wash period in control ACSF and remained significantly swollen ($*p < .05$, $**p < .01$ or $***p < .001$). The inability for AQP4 $^{-/-}$ astrocytes to recover their volume in the wash period resulted in significantly higher volume increases in the AQP4 $^{-/-}$ astrocytes relative to control during the second application of 10.5 mM $[K^+]_o$. These data suggest a possible role for AQP4 in water efflux from astrocytes rather than a route for water entry.

AQP4 = aquaporin 4.

and elevate glutamate uptake, either of which could modulate astrocyte swelling or volume regulatory mechanisms. Therefore, we performed experiments to determine the effects, if any, of neuronal firing on astrocyte swelling profiles in elevated $[K^+]_o$. We first performed current clamp recordings in CA1 pyramidal cells to determine the effect of 10.5 mM K^+ on neuronal V_m and action potential generation (Figure 8). During the baseline period in 2.5 mM K^+ ACSF, neurons rested at an average V_m of -67.2 ± 1.2 mV and fired only occasional action potentials. Application of 10.5 mM K^+ depolarized neurons to -48.3 ± 1.0 mV and generated action potentials at high frequency over 10 min (baseline frequency 0.022 Hz; 10.5 mM $[K^+]_o$ 0.759 Hz; $n = 11$ neurons, 11 slices). Neuronal V_m and firing frequency returned to near baseline levels upon return to 2.5 mM $[K^+]_o$. To address whether neuronal firing affects astrocyte swelling, we recorded astrocyte volume in 10.5 mM $[K^+]_o$ ACSF with and without TTX (Figure 8D to F). The presence of TTX did not alter the swelling responses of astrocytes in $[K^+]_o$. These findings suggest that (a) astrocyte swelling is not due to water movement occurring through activity-dependent glutamate uptake; and (b) possible stimulation of astrocytic receptors does not modulate the astrocyte swelling response in $[K^+]_o$.

Discussion

In this study, we found that elevated extracellular potassium (6.5, 10.5, or 26 mM) causes rapid (within 1 min) and significant astrocyte swelling, up to ~6, 7, and 15% above baseline volume, respectively, after 5 min.

Astrocytes recovered to baseline volume within 10 min after return to control 2.5 mM $[K^+]_o$ ACSF and again swelled to a similar extent upon reapplication of $[K^+]_o$ ACSF. Neuronal volume, on the other hand, remained largely unaffected by addition of K^+ to well above baseline values. These observations highlight the key role astrocytes play in regulating extracellular K^+ levels and provide direct evidence that astrocytes are the main cell type involved in cellular volume responses and associated constriction of the ECS in raised extracellular K^+ conditions. Astrocyte volume increases were significantly inhibited by 50 μ M ouabain, implicating the astrocyte NKA. BaCl $_2$ at 100 μ M had no effect on astrocyte volume increases, arguing against a role for Kir4.1. Inhibitors of other astrocytic channels and cotransporters often implicated in astrocyte swelling—including AQP4, NKCC1, and NBCe1—had no effect. Overall, our findings suggest that the NKA plays a key role in astrocyte volume expansion occurring in elevated extracellular K^+ conditions and provide further evidence that the astrocyte Na^+/K^+ pump isoform is unique in its sensitivity to rises in $[K^+]_o$.

The Na^+/K^+ pump inhibitor ouabain reduced the swelling of astrocytes to 0.90% above baseline after 5 min in 10.5 mM $[K^+]_o$ ACSF, compared with a 6.62% volume increase in $[K^+]_o$ alone. The slight amount of astrocyte swelling remaining in the presence of ouabain suggests an additional K^+ influx pathway may also play a small role in the K^+ clearance. Although the effects of 1 mM BaCl $_2$ support possible involvement of K^+ channels, BaCl $_2$ at this concentration nonselectively inhibits the Na^+/K^+ pump activity as previously reported (Walz et al., 1984). Application of 1 mM BaCl $_2$ together with

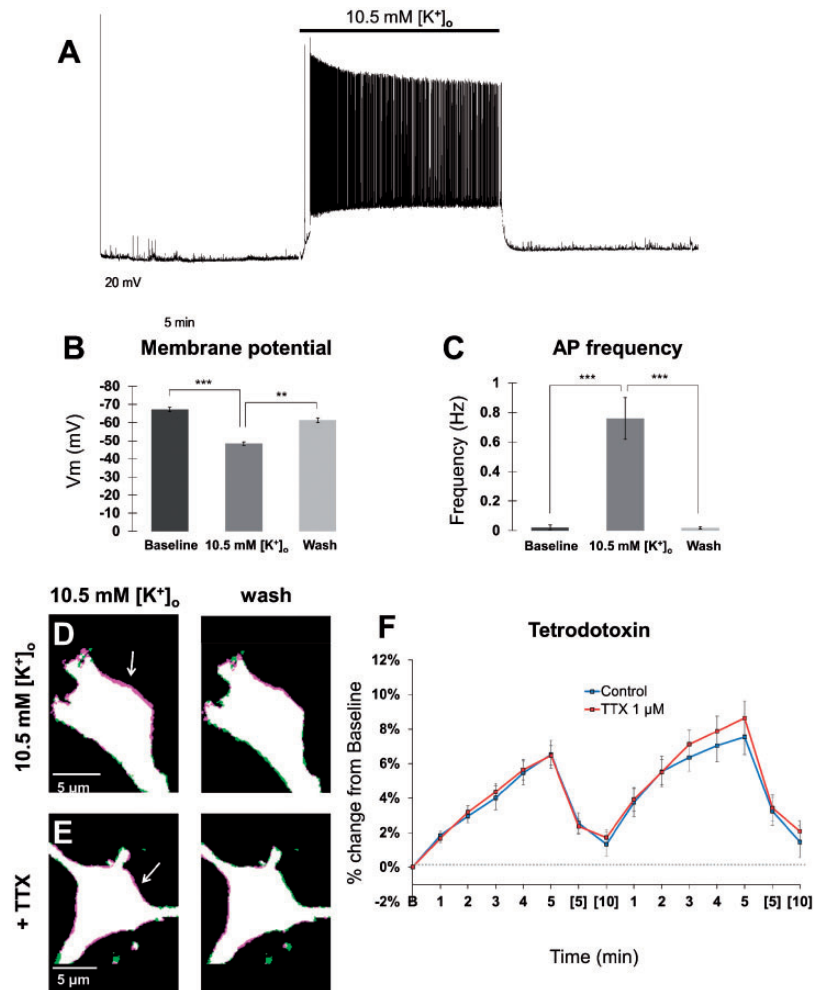


Figure 8. Block of Neuronal Firing Has No Effect on Astrocyte Swelling in Elevated Potassium. (A) Representative recording of a CA1 pyramidal neuron in 10.5 mM [K⁺]_o. Application of 10.5 mM [K⁺]_o depolarized the cell by ~25 mV and resulted in generation of frequent action potentials within ~30 s. In control ACSF (2.5 mM [K⁺]_o), action potentials were absent in this cell, both during the baseline and wash periods. (B) On average, neurons rested at -67.2 mV and depolarized to -48.3 mV in the presence of 10.5 mM [K⁺]_o. (C) Application of 10.5 mM [K⁺]_o significantly increased the frequency of action potentials in CA1 pyramidal cells on average. For (B) and (C), $n = 11$ neurons, $^{*}p < .01$, $^{***}p < .001$. Pseudocolor images of astrocytes (D, E) depict cell volume at baseline overlaid with images taken after 5 min in isoosmolar 10.5 mM [K⁺]_o (D) or 10.5 mM [K⁺]_o plus 1 μM TTX (E) (left panels). “Wash” images (right panels) show cell baseline volume overlaid with volume post-^{10.5 mM [K⁺]_o reperfusion in control ACSF. The magenta outline (arrows) shows expansion of the cell soma over baseline volume. (F) Coapplication of 1 μM TTX with 10.5 mM [K⁺]_o had no significant effect on astrocyte swelling compared with 10.5 mM [K⁺]_o alone (control $n = 8$; + TTX $n = 10$). TTX, like other antagonists, was applied 10 min prior to addition of 10.5 mM [K⁺]_o + TTX and was present throughout the electrophysiology recordings and imaging measurements. AP = action potential; TTX = tetrodotoxin.}

ouabain did not produce an additive effect, casting doubt on the specificity of barium for K⁺ channels at this concentration. Based on these results, our findings are consistent with a prominent role for the astrocyte NKA in ^{10.5 mM [K⁺]_o-induced astrocyte swelling. Our findings are in line with previous studies that have highlighted the unique Na⁺/K⁺ pump function of astrocytes and fit with the model of K⁺ clearance proposed by Ransom et al. (2000) from their work in the rat optic nerve. Here, they postulated (based upon their work as well as previous studies) that glial cells express an isoform of the}

NKA that is sensitive to changes in [K⁺]_o around the physiological concentration of 3 mM (i.e., low affinity) and that can adjust instantly to changes in [K⁺]_o. The optic nerve axons, on the other hand, were assumed to express an isoform of the NKA that is insensitive to changes in K⁺ but is sensitive to changes in [Na⁺]_o, similar to other neurons. Subsequent studies have largely corroborated this model. Cholet et al. (2002) found similar perisynaptic glial localization of the NKA α2 subunit and the astrocyte glutamate transporters glutamate-aspartate transporter (GLAST) and glutamate

transporter-1 (GLT-1) in the rat somatosensory cortex, indicating that $\alpha 2$ is predominantly glial. The MacAulay group then went on to show that (a) the $\alpha 2\beta 2$ isoform combination provides the low K^+ affinity and steep voltage sensitivity that render it kinetically geared to increase its activity in response to elevated extracellular K^+ (Larsen et al., 2014) and (b) that astrocytic $\alpha 2$ pairs mainly with the $\beta 2$ isoform at the protein level by proximity ligation assay (Stoica et al., 2017). Here, we demonstrate that the astrocyte NKA is functionally involved in K^+ uptake in raised extracellular K^+ conditions, generating astrocyte swelling and compression of the ECS. Lack of neuronal swelling in $^{\wedge}[K^+]_o$ may be due to their predominant expression of the $\alpha 1\beta 1$ isoform, which is largely insensitive to $[K^+]_o$ and responds instead to increases in intracellular Na^+ .

Using real-time volume measurements similar to those used here, previous studies have observed rapid neuronal swelling in elevated K^+ conditions raised to 26 mM or higher (Andrew et al., 2007; Zhou et al., 2010). Neuronal swelling correlates with SD, which often occurs in elevated extracellular K^+ conditions, but not necessarily by raised extracellular K^+ per se. The work of Zhou et al. (2010) was particularly helpful in this regard. They found that neuronal volume only changed if $^{\wedge}[K^+]_o$ evoked SD, but not when $^{\wedge}[K^+]_o$ failed to trigger SD. The two events were distinguishable by the intrinsic optical signals (IOS) they produced: Successful SD produced an initial fast transient peak in LT that appeared on top of a much slower IOS increase. When $^{\wedge}[K^+]_o$ failed to induce SD, there was no transient peak and no apparent propagation through the tissue; IOS showed only a gradual, nonpropagating increase which was instead due to more gradual slice swelling. In reports of successful induction of SD using high $[K^+]_o$, almost invariably some combination of the following are used: (a) physiological recording temperature, (b) very fast perfusion speeds (3–8 ml/min), and (c) focal application of very high $[K^+]_o$ to a small area of tissue using microfluidic chambers or iontophoresis. Zhou et al. (2010) found that slowing the perfusion rate alone was sufficient to prevent SD in 40 mM KCl at physiological temperature. Our combination of slow perfusion speeds (1.2–1.5 ml/min), recordings at room temperature, and bath application of K^+ were insufficient to promote SD, and therefore, cell swelling changes in 26 mM $^{\wedge}[K^+]_o$ were effectively isolated to astrocytes. The lower concentrations in the physiological range (6.5 and 10.5 mM) used in our studies were previously reported to be below the minimal K^+ concentration (~15 mM) needed to induce SD (Tang et al., 2014).

Elevated extracellular K^+ will depolarize neurons and increase neuronal action potential generation. Even a shift of 1–2 mM can lead to a significant increase in neuronal firing rates (Xie et al., 2012). We found that increasing $[K^+]_o$ to 10.5 mM greatly increases neuronal

firing on a timescale that correlates with astrocyte swelling. The elevated synaptic transmission in $^{\wedge}[K^+]_o$ could contribute to astrocyte swelling and/or volume regulation through uptake of released neurotransmitters into astrocytes, or activation of a broad array of astrocytic G protein-coupled receptors including the mGluRs, GABA_BRs, and P2YRs. Many GPCR subtypes have been reported to play a role in regulation of astrocyte transporters, K^+ channels, and cell volume (Mongin and Kimelberg, 2002; Takano et al., 2005; Gunnarson et al., 2008; Devaraju et al., 2013) and could potentially modify astrocyte homeostatic functions. Despite these possibilities, astrocyte volume responses in 10.5 mM $[K^+]_o$ were nearly identical in the presence of TTX compared with control. These findings suggest that, at least acutely, elevated neuronal firing does not significantly contribute to astrocyte volume responses in $^{\wedge}[K^+]_o$. It is possible that with more prolonged periods of neuronal firing, effects of astrocyte receptor activation on astrocyte volume responses or volume regulatory mechanisms could be uncovered.

Potassium-induced astrocyte swelling has been attributed to a host of different channels, pumps, and transporter systems in various studies. Early findings supported a role for NKCC1 (MacVicar et al., 2002; Su et al., 2002a, 2002b; Vázquez-Juárez et al., 2009). In many of these studies, the NKCC1 inhibitor bumetanide significantly attenuated astrocyte volume increases and reduced swelling-evoked release of osmolytes from astrocytes. However, most of these experiments were performed in culture and in the presence of up to 75 mM potassium. Astrocytes in culture possess unique characteristics and only marginally resemble astrocytes in intact brain tissue, as has been well documented previously (Cahoy et al., 2008; Fiacco et al., 2009; Larsen and MacAulay, 2017). Our findings *in situ* using a lower range of K^+ concentrations are supported by those of Larsen et al. (2014), who found that while NKCC1 was important for swelling of cultured astrocytes, it did not contribute to ECS reduction in intact brain tissue. Furthermore, the activity of NKCC1 during application of extreme concentrations (75 mM) of potassium is unlikely to simulate a physiologically relevant buildup of potassium in the ECS. Interestingly, a recent study reported that age may also be a factor in the composition and activity of membrane proteins responsible for volume regulation in astrocytes. In hippocampal slices exposed to 50 mM potassium, NKCC1 played a greater role in swelling of astrocytes from young animals in comparison to older mice (Kolenicova et al., 2020). Considering the lack of NKCC1 activity contributing to astrocyte swelling in our experiments, which were performed in P15 to P21 mice, it seems unlikely that NKCC1 would play a role in astrocyte swelling in slices

from older mice using the range of K^+ concentrations used in our study.

The inwardly rectifying potassium channel Kir4.1 is another target traditionally associated with astrocyte potassium buffering and associated volume changes. In hippocampal slices of this age, we and others have recorded significant Kir4.1 currents in astrocytes that are also blocked by $100\ \mu\text{M}$ BaCl_2 (Djukic et al., 2007; Devaraju et al., 2013). Multiple studies have demonstrated morphological and functional association of Kir4.1 with the glial-specific water channel AQP4 (Nagelhus et al., 1999; Wen et al., 1999; Manley et al., 2000; Nagelhus et al., 2004; Wurm et al., 2006; Strohschein et al., 2011). The working model, which has been supported by some findings, is that influx of potassium through Kir4.1 leads to corresponding inward water movement through AQP4, leading to glial swelling (Kitaura et al., 2009). In the present study, block of Kir4.1 by $100\ \mu\text{M}$ BaCl_2 had no effect on astrocyte swelling in $^{\wedge}[K^+]_o$, arguing against a role for Kir4.1 in removal of $[K^+]_o$ into astrocytes and subsequent volume changes. However, a recent immunohistochemical study demonstrated increased Kir4.1 signal in mouse hippocampus in P60 adult tissue, leaving open a possible role for Kir4.1 in astrocyte swelling in older mice (Moroni et al., 2015).

Like Kir4.1, AQP4 also appears unnecessary for astrocyte volume increases in $^{\wedge}[K^+]_o$. Our findings are in line with a number of other studies that have found minimal to no role for Kir4.1 or AQP4 in clearance of extracellular K^+ , cell swelling, or contraction of the ECS (D'Ambrosio et al., 2002; Haj-Yasein et al., 2011, 2012; Larsen et al., 2014; Toft-Bertelsen et al., 2020). For example, Haj-Yasein et al. (2011) reported that genetic deletion of Kir4.1 produced no change in stimulus-evoked shrinkage of the ECS. In subsequent work, the same group found that deletion of AQP4 actually increased ECS shrinkage, indicating a possible role for AQP4^{-/-} in astrocyte volume regulation (Haj-Yasein et al., 2012). This is consistent with our observations. In our previous work, we observed increased swelling of astrocytes in hippocampal slices from AQP4^{-/-} mice compared with control in a hypoosmolar cell swelling model (Murphy et al., 2017). In the present study, AQP4^{-/-} astrocytes exhibited a slower recovery to baseline volume during the wash period in-between $^{\wedge}[K^+]_o$ applications, resulting in increased peak volume during the second $^{\wedge}[K^+]_o$ application relative to control. Our data suggest that AQP4 is dispensable for astrocyte swelling, and in the absence of AQP4, astrocytes have impaired volume recovery. Based on both the present and past findings, we propose that during more elevated and sustained elevations in $[K^+]_o$, the main role of Kir4.1 and AQP4 is *redistribution* or *extrusion* of K^+ ions and water out of the astrocyte either into

the vasculature or into areas of lower $^{\wedge}[K^+]_o$, which aids in cell volume regulation. It is worth noting that our model exposes the tissue to potassium-enriched ACSF by bath application. Using this method, K^+ ions and water would presumably encounter most astrocytic compartments in a uniform and distributed manner. In contrast, many *in vivo* studies citing the importance of AQP4 in astrocyte swelling concern the volume transients through the endfeet of astrocytes abutting the vasculature (Manley et al., 2000; Amiry-Moghaddam et al., 2003; Badaut et al., 2011). Thus, the directionality of the water movement between vascular and interstitial compartments is an important consideration when comparing *in situ* to *in vivo* studies.

The NBCe1, monocarboxylate transporters MCT 1 and 4, and KCC are additional candidate pathways for astrocyte swelling in $^{\wedge}[K^+]_o$. Astrocytic K^+ -induced membrane depolarization has been shown to activate the NBCe1, resulting in influx of Na^+ and HCO_3^- and intracellular alkalization (reviewed in Deitmer and Rose, 2010). Two independent studies have supported a role for the NBCe1 in astrocyte swelling in conditions of elevated $^{\wedge}[K^+]_o$. Florence et al. (2012) observed astrocyte swelling 10 min after bath application of $5.5\ \text{mM}$ $^{\wedge}[K^+]_o$ using 2-photon imaging of fluorescently labeled astrocytes in rat hippocampal slices. The astrocyte swelling was significantly attenuated by DIDS and after incubating slices in HCO_3^- free ACSF. Later, Larsen and MacAulay (2017) also found a role for the NBCe1 in stimulation-induced ECS shrinkage. Inhibition of the NBCe1 by DIDS ($300\ \mu\text{M}$) reduced the ECS shrinkage by about 25%. In the present study, we found that $300\ \mu\text{M}$ DIDS had no effect on the amount of astrocyte swelling occurring in $^{\wedge}[K^+]_o$. Although used mainly with the intention of blocking the NBCe1, DIDS is a general anion exchange inhibitor and would therefore also be expected to at least partially block KCC at these concentrations (Malek et al., 2003; Delpire and Weaver, 2016). Furthermore, DIDS is also an effective antagonist of the MCTs at similar concentrations as those used here (Dimmer et al., 2000). Therefore, our findings provide evidence that there is limited to no involvement of NBCe1, KCC, or MCTs in the astrocyte swelling observed in $^{\wedge}[K^+]_o$ in our experiments.

We explored astrocyte swelling mechanisms using $^{\wedge}[K^+]_o$ of $10.5\ \text{mM}$. This is in line with peak K^+ during intense electrical stimulation and nearing ceiling levels during seizure. It is right near the theoretical peak of $[K^+]_o$ that the $\alpha 2\beta 2$ NKA isoform would saturate. Therefore, we cannot rule out possible involvement of other K^+ -influx pathways such as NKCC and KCC at higher concentrations of $[K^+]_o$. The KCCs in particular are generally outwardly directed, but during heavy extracellular K^+ loads such as during ischemia and SD, they may reverse and contribute to K^+ influx in pathological

situations (reviewed in Macaulay and Zeuthen, 2012). Although we did not induce SD in our experiments, 26 mM $[K^+]_o$ may be high enough to involve KCC-mediated K^+ influx. On the other end of the K^+ concentration range, Florence et al. (2012) found a role for the NBCe1 at much lower $[K^+]_o$ values of 5.5 mM. The NBCe1 might therefore contribute to volume responses at lower $[K^+]_o$ but is then phased out by the Na^+/K^+ pump as $[K^+]_o$ levels continue to rise. Another methodological difference between studies has to do with the duration of exposure of the tissue to $\hat{[K^+]_o}$. In the present study, astrocytes were imaged at 1-min intervals from the start of the $\hat{[K^+]_o}$ application for a total of 5 min prior to returning to baseline $[K^+]_o$. In contrast, Florence et al. (2012) took the first volume measurement 10 min after the initial exposure to $\hat{[K^+]_o}$ and continued recording for 40 min at 10-min intervals. Thus, the concentration as well as the duration of exposure to $\hat{[K^+]_o}$ may both be key variables influencing the role of different channels and transport pathways associated with astrocyte volume change.

In summary, our findings suggest that the NKA is the main contributor to potassium influx into astrocytes and the subsequent astrocyte swelling that occurs in elevated extracellular potassium conditions. Further study would be needed to pinpoint other candidate pathways responsible for the small amount of astrocyte swelling that remains during block of the NKA. A couple of key questions remain: (a) What is causing the cell swelling, and (b) how is the water getting into the cell? The NKA translocates 3 Na^+ out for every 2 K^+ in each cycle against the ion concentration gradients. Therefore, if water was simply following an osmotic gradient, water would move outward in the same direction as the net outward movement of ions. We propose a role for Cl^- ions similar to their involvement in neuronal swelling as reported by Rungta et al. (2015) in cytotoxic edema. Neuronal swelling is initiated by influx of Na^+ ions through activation of glutamate receptors and Na^+/K^+ pump reversal during energy failure. The neuronal depolarization activates voltage-gated Cl^- channels (SLC26A11) leading to accumulation of NaCl inside the cell, providing the osmotic imbalance leading to water entry. In the case of astrocytes, depolarization is triggered by the increase in $[K^+]_o$ which could activate voltage-gated chloride channels. Cl^- influx would accompany K^+ ions being pumped into the cell by the astrocytic NKA, resulting in accumulation of intracellular KCl and the osmotic imbalance leading to influx of water. Future studies would be necessary to identify candidate Cl^- channels responsible for the Cl^- influx.

As to how the water crosses the cell membrane, there is no evidence that the sodium-potassium pumps themselves are water permeable. Numerous studies have provided compelling evidence that AQP4 is not necessary for

astrocyte or neuronal swelling. Cotransporters and anion exchangers that have demonstrated water permeability, such as NKCC and KCC, have been shown to have limited to no role in the ECS dynamics or cell swelling following K^+ elevations within a physiological range. An intriguing candidate that warrants further investigation is the glutamate transporters. In addition to having an activity-dependent water permeability that can accompany glutamate uptake, the transporters also possess a parallel water pathway that is driven entirely by the osmotic gradient, analogous to the aquaporins (reviewed in MacAulay and Zeuthen, 2010). Although the unit water permeability is manyfold smaller than that of AQP4, these are among the most abundantly expressed proteins in astrocytes and are localized throughout the astrocyte membrane including the perisynaptic region. Previous work has demonstrated almost complete codistribution of the astrocytic NKA $\alpha 2$ subunit and the glutamate transporters GLAST and GLT-1 in glial leaflets surrounding dendritic spines and the dendritic and/or axonal elements at the ultrastructural level (Cholet et al., 2002). The glutamate transporters may therefore provide the passive water entry route responsible for astrocyte swelling in elevated $[K^+]_o$ conditions, in a manner reminiscent of what has been previously ascribed to AQP4.

Summary

- Elevated extracellular K^+ ($\hat{[K^+]_o}$) results in astrocyte-specific volume increases, with no change in neuronal volume.
- Astrocyte volume increases in $\hat{[K^+]_o}$ are inhibited by ouabain, implicating the Na^+/K^+ ATPase.
- Astrocyte swelling in $\hat{[K^+]_o}$ is not mediated by AQP4.

Author Contributions

E. W., T. R. M., N. C., and D. D. were involved in data generation and writing early and later portions of the article. C. M., J. D., G. Y., A. S., S. G., and C. A. performed many of the imaging experiments and subsequent analysis of data and contributed their ideas to the overall progress of the project. M. A. ran statistical analysis, prepared all figures, and edited the article. A. B. performed electrophysiology recordings in neurons. E. W. took lead in the submission and final editing process and wrote initial portions of the article. D. K. B. contributed conceptually to the overall work. T. A. F. was the lead in the initial planning of the work, overall research direction, experimental design, and wrote large portions of the article.

Declaration of Conflicting Interests


The author(s) declared no potential conflicts of interest with respect to the research, authorship, and/or publication of this article.

Funding

The author(s) disclosed receipt of the following financial support for the research, authorship, and/or publication of this article: This work was supported by the National Institutes of Health National Institute of Neurological Disorders and Stroke (grant numbers R01NS082570 and R21NS109918) and a UCR Academic Senate Committee on Research grant.

ORCID iDs

Erin Walch  <https://orcid.org/0000-0002-7809-9632>

Thomas R. Murphy  <https://orcid.org/0000-0002-2168-0602>

Jordan Donohue  <https://orcid.org/0000-0003-2997-5525>

Todd A. Fiacco  <https://orcid.org/0000-0003-1927-5349>

References

- Amiry-Moghaddam, M., Otsuka, T., Hurn, P. D., Traystman, R. J., Haug, F. M., Froehner, S. C., Adams, M. E., Neely, J. D., Agre, P., Ottersen, O. P. T., & Bhardwaj, A. (2003). An alpha-syntrophin-dependent pool of AQP4 in astroglial end-feet confers bidirectional water flow between blood and brain. *Proc Natl Acad Sci U S A*, *100*(4), 2106–2111.
- Andrew, R. D., Labron, M. W., Boehnke, S. E., Carnduff, L., & Kirov, S. A. (2007). Physiological evidence that pyramidal neurons lack functional water channels. *Cereb Cortex*, *17*(4), 787–802.
- Andrew, R. D., & MacVicar, B. A. (1994). Imaging cell volume changes and neuronal excitation in the hippocampal slice. *Neuroscience*, *62*(2), 371–383.
- Badaut, J., Ashwal, S., Adami, A., Tone, B., Recker, R., Spagnoli, D., Ternon, B., & Obenaus, A. (2011). Brain water mobility decreases after astrocytic aquaporin-4 inhibition using RNA interference. *J Cereb Blood Flow Metab*, *31*(3), 819–831.
- Benesova, J., Rusnakova, V., Honsa, P., Pivonkova, H., Dzamba, D., Kubista, M., & Anderova, M. (2012). Distinct expression/function of potassium and chloride channels contributes to the diverse volume regulation in cortical astrocytes of GFAP/EGFP mice. *PLoS One*, *7*(1), e29725.
- Benham, C. D., Bolton, T. B., Lang, R. J., & Takewaki, T. (1985). The mechanism of action of Ba²⁺ and TEA on single Ca²⁺-activated K⁺ channels in arterial and intestinal smooth muscle cell membranes. *Pflügers Arch*, *403*(2), 120–127.
- Binder, D. K., Papadopoulos, M. C., Haggie, P. M., & Verkman, A. S. (2004). In vivo measurement of brain extracellular space diffusion by cortical surface photobleaching. *J Neurosci*, *24*(37), 8049–8056.
- Cahoy, J. D., Emery, B., Kaushal, A., Foo, L. C., Zamanian, J. L., Christopherson, K. S., Xing, Y., Lubischer, J. L., Krieg, P. A., Krupenko, S. A., Thompson, W. J., & Barres, B. A. (2008). A transcriptome database for astrocytes, neurons, and oligodendrocytes: A new resource for understanding brain development and function. *J Neurosci*, *28*(1), 264–278.
- Cholet, N., Pellerin, L., Magistretti, P. J., & Hamel, E. (2002). Similar perisynaptic glial localization for the Na⁺,K⁺-ATPase alpha 2 subunit and the glutamate transporters GLAST and GLT-1 in the rat somatosensory cortex. *Cereb Cortex*, *12*(5), 515–525.
- Connors, N., Adams, M., Froehner, S., & Kofuji, P. (2004). The potassium channel Kir4.1 associates with the dystrophin-glycoprotein complex via alpha-syntrophin in glia. *J Biol Chem*, *279*(27), 28387–28392.
- D'Ambrosio, R., Gordon, D. S., & Winn, H. R. (2002). Differential role of KIR channel and Na⁽⁺⁾/K⁽⁺⁾-pump in the regulation of extracellular K⁽⁺⁾ in rat hippocampus. *J Neurophysiol*, *87*(1), 87–102.
- Davies, M. L., Kirov, S. A., & Andrew, R. D. (2007). Whole isolated neocortical and hippocampal preparations and their use in imaging studies. *J Neurosci Methods*, *166*(2), 203–216.
- Deitmer, J. W., & Rose, C. R. (2010). Ion changes and signaling in perisynaptic glia. *Brain Res Rev*, *63*(1–2), 113–129.
- Delpire, E., & Weaver, C. D. (2016). Challenges of finding novel drugs targeting the K-Cl cotransporter. *ACS Chem Neurosci*, *7*(12), 1624–1627.
- Devaraju, P., Sun, M., Myers, T., Lauderdale, K., & Fiacco, T. (2013). Astrocytic group I mGluR-dependent potentiation of astrocytic glutamate and potassium uptake. *J Neurophysiol*, *109*(9), 2404–2414.
- Dimmer, K. S., Friedrich, B., Lang, F., Deitmer, J. W., & Broer, S. (2000). The low-affinity monocarboxylate transporter MCT4 is adapted to the export of lactate in highly glycolytic cells. *Biochem J*, *350*(Pt 1), 219–227.
- Djukic, B., Casper, K. B., Philpot, B. D., Chin, L. S., & McCarthy, K. D. (2007). Conditional knock-out of Kir4.1 leads to glial membrane depolarization, inhibition of potassium and glutamate uptake, and enhanced short-term synaptic potentiation. *J Neurosci*, *27*(42), 11354–11365.
- Elwej, A., Chaabane, M., Ghorbel, I., Chelly, S., Boudawara, T., & Zeghal, N. (2017). Effects of barium graded doses on redox status, membrane bound ATPases and histomorphological aspect of the liver in adult rats. *Toxicol Mech Methods*, *27*(9), 677–686.
- Elwej, A., Ghorbel, I., Chaabane, M., Soudani, N., Mnif, H., Boudawara, T., Zeghal, N., & Sefi, M. (2018). Zinc and selenium modulate barium-induced oxidative stress, cellular injury and membrane-bound ATPase in the cerebellum of adult rats and their offspring during late pregnancy and early postnatal periods. *Arch Physiol Biochem*, *124*(3), 237–246.
- Feng, G., Mellor, R., Bernstein, M., Keller-Peck, C., Nguyen, Q., Wallace, M., Nerbonne, J., Lichtman, J., & Sanes, J. (2000). Imaging neuronal subsets in transgenic mice expressing multiple spectral variants of GFP. *Neuron*, *28*(1), 41–51.
- Fiacco, T. A., Agulhon, C., & McCarthy, K. D. (2009). Sorting out astrocyte physiology from pharmacology. *Annu Rev Pharmacol Toxicol*, *49*, 151–174.
- Florence, C. M., Baillie, L. D., & Mulligan, S. J. (2012). Dynamic volume changes in astrocytes are an intrinsic phenomenon mediated by bicarbonate ion flux. *PLoS One*, *7*(11), e51124.
- Gunnarson, E., Zelenina, M., Axehult, G., Song, Y., Bondar, A., Krieger, P., Brismar, H., Zelenin, S., & Aperia, A. (2008). Identification of a molecular target for glutamate regulation of astrocyte water permeability. *Glia*, *56*(6), 587–596.

- Haj-Yasein, N. N., Jensen, V., Østby, I., Omholt, S. W., Voipio, J., Kaila, K., Ottersen, O. P., Hvalby, Ø., & Nagelhus, E. A. (2012). Aquaporin-4 regulates extracellular space volume dynamics during high-frequency synaptic stimulation: A gene deletion study in mouse hippocampus. *Glia*, *60*(6), 867–874.
- Haj-Yasein, N. N., Jensen, V., Vindedal, G. F., Gundersen, G. A., Klungland, A., Ottersen, O. P., Hvalby, O., & Nagelhus, E. A. (2011). Evidence that compromised K⁺ spatial buffering contributes to the epileptogenic effect of mutations in the human Kir4.1 gene (KCNJ10). *Glia*, *59*(11), 1635–1642.
- Hille, B. (1978). Ionic channels in excitable membranes. Current problems and biophysical approaches. *Biophys J*, *22*(2), 283–294.
- Jayakumar, A. R., & Norenberg, M. D. (2010). The Na-K-Cl Co-transporter in astrocyte swelling. *Metab Brain Dis*, *25*(1), 31–38.
- Kalsi, A. S., Greenwood, K., Wilkin, G., & Butt, A. M. (2004). Kir4.1 expression by astrocytes and oligodendrocytes in CNS white matter: A developmental study in the rat optic nerve. *J Anat*, *204*(6), 475–485.
- Kitaura, H., Tsujita, M., Huber, V. J., Kakita, A., Shibuki, K., Sakimura, K., Kwee, I. L., & Nakada, T. (2009). Activity-dependent glial swelling is impaired in aquaporin-4 knockout mice. *Neurosci Res*, *64*(2), 208–212.
- Kofuji, P., & Newman, E. A. (2004). Potassium buffering in the central nervous system. *Neuroscience*, *129*(4), 1045–1056.
- Kolenicova, D., Tureckova, J., Pukajova, B., Harantova, L., Kriska, J., Kirdajova, D., Vorisek, I., Kamenicka, M., Valihrach, L., Androvic, P., Kubista, M., Vargova, L., & Anderova, M. (2020). High potassium exposure reveals the altered ability of astrocytes to regulate their volume in the aged hippocampus of GFAP/EGFP mice. *Neurobiol Aging*, *86*, 162–181.
- Larsen, B. R., Assentoft, M., Cotrina, M. L., Hua, S. Z., Nedergaard, M., Kaila, K., Voipio, J., & MacAulay, N. (2014). Contributions of the Na⁺/K⁺-ATPase, NKCC1, and Kir4.1 to hippocampal K⁺ clearance and volume responses. *Glia*, *62*(4), 608–622.
- Larsen, B. R., & MacAulay, N. (2017). Activity-dependent astrocyte swelling is mediated by pH-regulating mechanisms. *Glia*, *65*(10), 1668–1681.
- Larsen, B. R., Stoica, A., & MacAulay, N. (2016). Managing brain extracellular K(+) during neuronal activity: The physiological role of the Na(+)/K(+)-ATPase subunit isoforms. *Front Physiol*, *7*, 141.
- Lichter-Konecki, U., Mangin, J., Gordish-Dressman, H., Hoffman, E., & Gallo, V. (2008). Gene expression profiling of astrocytes from hyperammonemic mice reveals altered pathways for water and potassium homeostasis in vivo. *Glia*, *56*(4), 365–377.
- Lu, J., & Boron, W. F. (2007). Reversible and irreversible interactions of DIDS with the human electrogenic Na/HCO₃ cotransporter NBCe1-A: Role of lysines in the KKMVK motif of TM5. *Am J Physiol Cell Physiol*, *292*(5), C1787–1798.
- MacAulay, N., & Zeuthen, T. (2010). Water transport between CNS compartments: Contributions of aquaporins and cotransporters. *Neuroscience*, *168*(4), 941–956.
- MacAulay, N., & Zeuthen, T. (2012). Glial K⁺ clearance and cell swelling: Key roles for cotransporters and pumps. *Neurochem Res*, *37*(11), 2299–2309.
- MacVicar, B. A., Feighan, D., Brown, A., & Ransom, B. (2002). Intrinsic optical signals in the rat optic nerve: Role for K⁺ uptake via NKCC1 and swelling of astrocytes. *Glia*, *37*(2), 114–123.
- Malek, S. A., Coderre, E., & Stys, P. K. (2003). Aberrant chloride transport contributes to anoxic/ischemic white matter injury. *J Neurosci*, *23*(9), 3826–3836.
- Manley, G. T., Fujimura, M., Ma, T. H., Noshita, N., Filiz, F., Bollen, A. W., Chan, P., & Verkman, A. S. (2000). Aquaporin-4 deletion in mice reduces brain edema after acute water intoxication and ischemic stroke. *Nat Med*, *6*(2), 159–163.
- Melone, M., Ciriachi, C., Pietrobon, D., & Conti, F. (2019). Heterogeneity of astrocytic and neuronal GLT-1 at cortical excitatory synapses, as revealed by its colocalization with Na⁺/K⁺-ATPase alpha isoforms. *Cereb Cortex*, *29*(8), 3331–3350.
- Miller, C., Latorre, R., & Reisin, I. (1987). Coupling of voltage-dependent gating and Ba⁺⁺ block in the high-conductance, Ca⁺⁺-activated K⁺ channel. *J Gen Physiol*, *90*(3), 427–449.
- Mongin, A. A., Aksentsev, S. L., Orlov, S. N., Slepko, N. G., Kozlova, M. V., Maximov, G. V., & Konev, S. V. (1994). Swelling-induced K⁺ influx in cultured primary astrocytes. *Brain Res*, *655*(1–2), 110–114.
- Mongin, A. A., & Kimelberg, H. K. (2002). ATP potently modulates anion channel-mediated excitatory amino acid release from cultured astrocytes. *Am J Physiol Cell Physiol*, *283*(2), C569–578.
- Moroni, R. F., Inverardi, F., Regondi, M. C., Pennacchio, P., & Frassoni, C. (2015). Developmental expression of Kir4.1 in astrocytes and oligodendrocytes of rat somatosensory cortex and hippocampus. *Int J Dev Neurosci*, *47*(Pt B), 198–205.
- Murphy, T. R., Davila, D., Cuvelier, N., Young, L. R., Lauderdale, K., Binder, D. K., & Fiocco, T. A. (2017). Hippocampal and cortical pyramidal neurons swell in parallel with astrocytes during acute hypoosmolar stress. *Front Cell Neurosci*, *11*, 275.
- Nagelhus, E. A., Horio, Y., Inanobe, A., Fujita, A., Haug, F. M., Nielsen, S., Kurachi, Y., & Ottersen, O. P. (1999). Immunogold evidence suggests that coupling of K⁺ siphoning and water transport in rat retinal Müller cells is mediated by a coenrichment of Kir4.1 and AQP4 in specific membrane domains. *Glia*, *26*(1), 47–54.
- Nagelhus, E. A., Mathiisen, T. M., & Ottersen, O. P. (2004). Aquaporin-4 in the central nervous system: Cellular and subcellular distribution and coexpression with KIR4.1. *Neuroscience*, *129*(4), 905–913.
- Nagelhus, E. A., Veruki, M. L., Torp, R., Haug, F. M., Laake, J. H., Nielsen, S., Agre, P., & Ottersen, O. P. (1998). Aquaporin-4 water channel protein in the rat retina and

- optic nerve: Polarized expression in Muller cells and fibrous astrocytes. *J Neurosci*, 18(7), 2506–2519.
- Nielsen, S., Nagelhus, E. A., Amiry-Moghaddam, M., Bourque, C., Agre, P., & Ottersen, O. P. (1997). Specialized membrane domains for water transport in glial cells: High-resolution immunogold cytochemistry of aquaporin-4 in rat brain. *J Neurosci*, 17(1), 171–180.
- Pasantes-Morales, H., & Schousboe, A. (1989). Release of taurine from astrocytes during potassium-evoked swelling. *Glia*, 2(1), 45–50.
- Ransom, B. R., Yamate, C. L., & Connors, B. W. (1985). Activity-dependent shrinkage of extracellular space in rat optic nerve: A developmental study. *J Neurosci*, 5(2), 532–535.
- Ransom, C. B., Ransom, B. R., & Sontheimer, H. (2000). Activity-dependent extracellular K⁺ accumulation in rat optic nerve: The role of glial and axonal Na⁺ pumps. *J Physiol*, 522(Pt 3), 427–442.
- Risher, W. C., Andrew, R. D., & Kirov, S. A. (2009). Real-time passive volume responses of astrocytes to acute osmotic and ischemic stress in cortical slices and in vivo revealed by two-photon microscopy. *Glia*, 57(2), 207–221.
- Rudy, B. (1988). Diversity and ubiquity of K channels. *Neuroscience*, 25(3), 729–749.
- Rungta, R. L., Choi, H. B., Tyson, J. R., Malik, A., Dissing-Olesen, L., Lin, P. J. C., Cain, S. M., Cullis, P. R., Snutch, T. P., & MacVicar, B. A. (2015). The cellular mechanisms of neuronal swelling underlying cytotoxic edema. *Cell*, 161(3), 610–621.
- Schnell, C., Shahmoradi, A., Wichert, S., Mayerl, S., Hagos, Y., Heuer, H., Rossner, M., & Hulsmann, S. (2015). The multi-specific thyroid hormone transporter OATP1C1 mediates cell-specific sulforhodamine 101-labeling of hippocampal astrocytes. *Brain Struct Funct*, 220(1), 193–203.
- Steffensen, A. B., Sword, J., Croom, D., Kirov, S. A., & MacAulay, N. (2015). Chloride cotransporters as a molecular mechanism underlying spreading depolarization-induced dendritic beading. *J Neurosci*, 35(35), 12172–12187.
- Stoica, A., Larsen, B. R., Assentoft, M., Holm, R., Holt, L. M., Vilhardt, F., Vilsen, B., Lykke-Hartmann, K., Olsen, M. L., & MacAulay, N. (2017). The alpha2beta2 isoform combination dominates the astrocytic Na⁺/K⁺-ATPase activity and is rendered nonfunctional by the alpha2.G301R familial hemiplegic migraine type 2-associated mutation. *Glia*, 65(11), 1777–1793.
- Strohschein, S., Huttmann, K., Gabriel, S., Binder, D. K., Heinemann, U., & Steinhauser, C. (2011). Impact of aquaporin-4 channels on K⁺ buffering and gap junction coupling in the hippocampus. *Glia*, 59(6), 973–980.
- Su, G., Kintner, D. B., Flagella, M., Shull, G. E., & Sun, D. D. (2002a). Astrocytes from Na⁺-K⁺-Cl⁻-cotransporter-null mice exhibit absence of swelling and decrease in EAA release. *Am J Physiol Cell Physiol*, 282(5), C1147–C1160.
- Su, G., Kintner, D. B., & Sun, D. D. (2002b). Contribution of Na⁺-K⁺-Cl⁻ cotransporter to high- K⁺ (o)-induced swelling and EAA release in astrocytes. *Am J Physiol Cell Physiol*, 282(5), C1136–C1146.
- Sword, J., Croom, D., Wang, P. L., Thompson, R. J., & Kirov, S. A. (2017). Neuronal pannexin-1 channels are not molecular routes of water influx during spreading depolarization-induced dendritic beading. *J Cereb Blood Flow Metab*, 37(5), 1626–1633.
- Takano, T., Kang, J., Jaiswal, J. K., Simon, S. M., Lin, J. H., Yu, Y., Li, Y., Yang, J., Dienel, G., Zielke, H. R., & Nedergaard, M. (2005). Receptor-mediated glutamate release from volume sensitive channels in astrocytes. *Proc Natl Acad Sci U S A*, 102(45), 16466–16471. USA
- Tang, Y. T., Mendez, J. M., Theriot, J. J., Sawant, P. M., Lopez-Valdes, H. E., Ju, Y. S., & Brennan, K. C. (2014). Minimum conditions for the induction of cortical spreading depression in brain slices. *J Neurophysiol*, 112(10), 2572–2579.
- Toft-Bertelsen, T. L., Larsen, B. R., Christensen, S. K., Khandelia, H., Waagepetersen, H. S., & MacAulay, N. (2020). Clearance of activity-evoked K⁽⁺⁾ transients and associated glia cell swelling occur independently of AQP4: A study with an isoform-selective AQP4 inhibitor. *Glia*. Advance online publication. <https://doi.org/10.1002/glia.23851>
- Traynelis, S. F., & Dingledine, R. (1988). Potassium-induced spontaneous electrographic seizures in the rat hippocampal slice. *J Neurophysiol*, 59(1), 259–276.
- Traynelis, S. F., Dingledine, R., McNamara, J. O., Butler, L., & Rigsbee, L. (1989). Effect of kindling on potassium-induced electrographic seizures in vitro. *Neurosci Lett*, 105(3), 326–332.
- Vázquez-Juárez, E., Hernández-Benítez, R., López-Domínguez, A., & Pasantes-Morales, H. (2009). Thrombin potentiates D-aspartate efflux from cultured astrocytes under conditions of K⁺ homeostasis disruption. *J Neurochem*, 111(6), 1398–1408.
- Walter, S. J., Shirley, D. G., Folkard, E. J., & Unwin, R. J. (2001). Effects of the potassium channel blocker barium on sodium and potassium transport in the rat loop of henle in vivo. *Exp Physiol*, 86(4), 469–474.
- Walz, W. (1992). Mechanism of rapid K⁽⁺⁾-induced swelling of mouse astrocytes. *Neurosci Lett*, 135(2), 243–246.
- Walz, W. (2000). Role of astrocytes in the clearance of excess extracellular potassium. *Neurochem Int*, 36(4–5), 291–300.
- Walz, W., & Hinks, E. C. (1985). Carrier-mediated KCl accumulation accompanied by water movements is involved in the control of physiological K⁺ levels by astrocytes. *Brain Res*, 343(1), 44–51.
- Walz, W., Shargool, M., & Hertz, L. (1984). Barium-induced inhibition of K⁺ transport mechanisms in cortical astrocytes—its possible contribution to the large Ba²⁺-evoked extracellular K⁺ signal in brain. *Neuroscience*, 13(3), 945–949.
- Wen, H., Nagelhus, E. A., Amiry-Moghaddam, M., Agre, P., Ottersen, O. P., & Nielsen, S. (1999). Ontogeny of water transport in rat brain: Postnatal expression of the aquaporin-4 water channel. *Eur J Neurosci*, 11(3), 935–945.
- Wurm, A., Pannicke, T., Iandiev, I., Wiedemann, P., Reichenbach, A., & Bringmann, A. (2006). The

- developmental expression of K⁺ channels in retinal glial cells is associated with a decrease of osmotic cell swelling. *Glia*, 54(5), 411–423.
- Xie, A., Lauderdale, K., Murphy, T., Myers, T., & Fiacco, T. (2014). Inducing plasticity of astrocytic receptors by manipulation of neuronal firing rates. *J Vis Exp*, 20(85), 51458.
- Xie, A. X., Sun, M. Y., Murphy, T., Lauderdale, K., Tiglao, E., & Fiacco, T. A. (2012). Bidirectional scaling of astrocytic metabotropic glutamate receptor signaling following long-term changes in neuronal firing rates. *PLoS One*, 7(11), e49637.
- Zhou, N., Gordon, G., Feighan, D., & MacVicar, B. (2010). Transient swelling, acidification, and mitochondrial depolarization occurs in neurons but not astrocytes during spreading depression. *Cereb Cortex*, 20(11), 2614–2624.